Periodic and Guiding Structures at Microwave Frequencies*

A. F. HARVEY†

Summary—**The paper reviews the properties of periodic and guiding structures which now play an important part in the operation of components, antennas, electron tubes and low-noise amplifiers. An account is first given of dispersive propagation in periodic-loaded lines, showing how the frequency characteristic breaks into pass and stop bands. The formation of forward- and backward-space harmonics and the effect of systematic modification of loading are examined. A description is then given of the various types of surface-wave structures including dielectric rods, dielectric-clad metals, and corrugated surfaces, as well as surface wave instruments and circuits. Practical slow-wave structures such as ladder lines, coupled cavities and helices are finally treated. The survey concludes with a bibliography.**

List of Principal Symbols

(Rationalized mks Units are Used Unless Otherwise Indicated)

b = Linear dimension, meters.
c = Speed of light in vacuo = 2.997929×10^{8} meters per second.
C = Capacitance, farads.
d = Linear dimension, meters.
E = Electric field, volts per meter.
H = Magnetic field intensity, ampere turns per meter ($=4\pi\times10^{-3}$ oersted).
$H_n^{(1)}$ = Hankel function of the first kind and nth order.
$H_n^{(2)}$ = Hankel function of the second kind and nth order.
j = Operator, 90° rotational = $\sqrt{-1}$.
J_n = Bessel function of the first kind and nth order.
l = Length, meters.
l = Suffix for long.
L = Inductance, henry.
m = Integer.
n = Integer.
N = Number of resonators or elements.
p = Pitch of periodic structure, meters.
P = Power, watts.
Q_u = Unloaded Q factor.
r = Radial coordinate or suffix.
r_h = Radius of helix, meters.
r_1 = Radius of rod, meters.
R_s = Surface resistance, ohms.
s = Suffix for short.
t = Time, seconds.
u = Radial propagation coefficient = $a+jb$.
v_g = Group velocity of wave = $d\omega/d\beta$ meters per second.
v_p = Phase velocity of wave = ω/β meters per second.
w = Linear dimension, meters.
W_s = Total average stored energy per unit length, joules per meter.
x = Linear coordinate, meters or suffix.
X_s = Surface reactance, ohms.
y = Linear coordinate, meters or suffix.
Y_n = Bessel function of the second kind and nth order.
Y_0 = Characteristic admittance of transmission line, mhos.
Y_1 = Admittance of stub, mhos.
z = Axial linear coordinate, meters or suffix.
Z_c = Coupling impedance of circuit, ohms.
Z_0 = Characteristic impedance of transmission line, ohms.
Z_s = Surface impedance = R_s+jX_s ohms.
Z_{sh} = Shunt impedance of circuit, ohms per meter.
Z_w = Wave impedance of free space = 377 ohms.
Z_1 = Impedance of loading element, ohms.
α = Attenuation coefficient, nepers per meter.
β = Phase-change coefficient = $2\pi/\lambda_g$, radians per meter.
β_n = Value of β for nth space harmonic.
β_w = Value of β in free space.
γ = Propagation coefficient = $\alpha+j\beta$.
γ_n = Value of γ for nth space harmonic.
δ = Dielectric loss angle.
δ_s = Skin depth in a conductor = $2/(\omega\mu\mu_0\sigma)^{1/2}$ meters.
ϵ = Dielectric constant.
ϵ_0 = Electric space constant, $(1/36\pi)10^{-9}$ farads per meter.
θ = Angular coordinate or suffix.
λ = Free-space wavelength, meters.
λ_c = Cutoff wavelength of waveguide, meters.
λ_g = Guide wavelength, meters.
μ = Relative permeability.
μ_0 = Magnetic space constant, $4\pi\times10^{-7}$ henry per meter.
ρ = Amplitude reflection coefficient.
σ = Conductivity, mhos per meter.
ϕ = Angular coordinate or suffix.
ψ_h = Pitch angle of helix.
ω = Angular frequency, radians per second.

* Manuscript received by the PGMTT, January 2, 1959; revised manuscript received July 27, 1959.
† Royal Radar Establishment, Malvern, Worcester, Eng.

Waves in Periodically-Loaded Lines

Dispersion

The propagation characteristics of a transmission line are modified [39] when the line is loaded with reactances connected in series or parallel, and spaced at regular intervals. The analysis of such periodic structures, familiar [30] in many branches of science, has been extended [50], [167], [233] to microwave transmission lines. An equivalent circuit treatment reveals a qualitative description of the various phenomena, providing a basis for exact analysis using Maxwell's theory.

Propagation along a transmission line, loaded as shown in Fig. 1, may be analyzed by Floquet's theorem [30], [233] which states that for a given mode of oscillation and frequency the wave function is multiplied by a constant complex factor exp $(-\gamma p)$ on moving along the structure by one section or period. For propagation along the z-axis, the wave function can be written in the general form $\exp -(\gamma+2\pi nj/p)z$. It can be shown that in a structure without energy dissipation γ must be real or imaginary. If real, the exponentials for each value of n decrease with increasing z and attenuated waves result. If, on the other hand, γ is imaginary, putting

$$\beta_n = \beta_0 + 2\pi n/p, \tag{1}$$

the wave function becomes exp $j(\omega t-\beta_n z)$, on inclusion of the time dependent term. This represents a progressive wave with angular frequency ω and wavelength $2\pi/\beta_n$, travelling along the z-axis with phase velocity $v_{pn}=\omega/\beta_n$.

The loaded line may be considered as a series of sections, each consisting of a portion of line of characteristic impedance Z_0 and a lumped impedance Z_1. The phase change across a section AC consists of the sum of the phase changes along a portion of line AB and across the lumped impedance BC. The equations of the frequency characteristics of this infinite loaded line may be determined by the usual analysis [271] of ladder lines. The phase change along a length of transmission line is $2\pi p/\lambda$, while the total phase change per section is $\beta_n p$ or $2\pi p/\lambda_g$ when n is considered zero. It can then be shown [167] that

$$\cos\frac{2\pi p}{\lambda_g} = \cos\frac{2\pi p}{\lambda} + j\frac{Z_1}{2Z_0}\sin\frac{2\pi p}{\lambda} \tag{2}$$

is the equation of the frequency characteristic. For a line loaded with series inductances L,

$$Z_1 = j\omega L \tag{3}$$

and the resulting (2) with $\omega L \simeq Z_0$ is plotted in Fig. 2. It will be seen that as ω is increased from zero to about two-thirds of $\pi c/p$ the value of β increases from zero to π/p. At this higher frequency, reflections set up at the inductors add in phase, resulting in a standing wave on the line with current antinodes at the inductors. For higher frequencies a stop band occurs, the wave down the line being attenuated by successive reflections at the inductors while the total phase change remains constant at the value π. For smaller or larger values of L, the curves have similar shapes but follow the $v_p=c$ line to higher or lower frequencies, respectively. The curves always have zero slope at cutoff and propagation is possible at zero frequency. A second pass band begins when the phase change across each portion of the line (not including the inductor) becomes π; *i.e.*, when ω becomes $\pi c/p$. At this frequency there is no phase change across the inductor, a standing wave being produced with nodes at the inductor. With further increase in frequency, the phase constant increases until the phase change across each section of the line becomes 2π when a further stop band occurs. The widths of successive stop bands increase with frequency since they are dependent on the reactance ωL of the inductor. It will be seen that the phase velocity given by ω/β is less than c, except in the special case of standing waves with current nodes at the inductors when, as may be expected, it is equal to c.

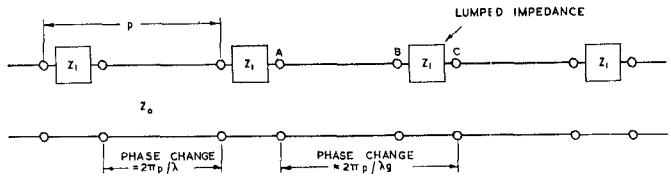

Fig. 1—Line loaded with lumped impedance.

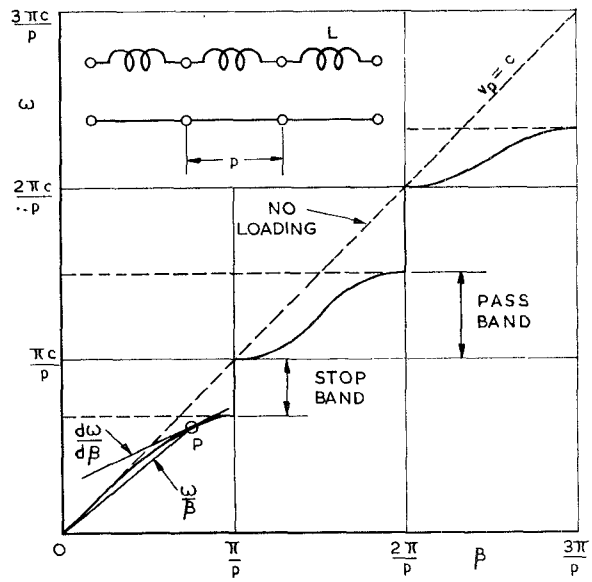

Fig. 2—Frequency characteristic for inductively loaded line.

For a line loaded with series capacitances C,

$$Z_1 = 1/j\omega C \tag{4}$$

and the resulting (2) with $(1/\omega C)\simeq 3Z_0$ is plotted in Fig. 3. Once again a series of stop and pass bands is obtained but in this case the widths of the stop bands

decrease with increasing frequency. The phase change across the capacitor is such that the phase velocity is greater than c, except when a standing wave with nodes at the capacitors occurs when it is equal to c. It should be observed that the transmission line now has a cutoff frequency below which no propagation occurs. The general shape of the curves is the same for other values of C, tending to the $v_p = c$ line for C large and to horizontal lines representing no propagation for C small. These dispersion curves for series capacitance are identical with those for shunt inductance loading while, by the principle of duality, the curves for shunt capacitance are identical with those already shown for series inductance.

Microwave transmission lines are often loaded with resonant circuits such as, for example, series stubs. If l is the length and Z_{01} is the characteristic impedance of such a stub, the loading impedance is

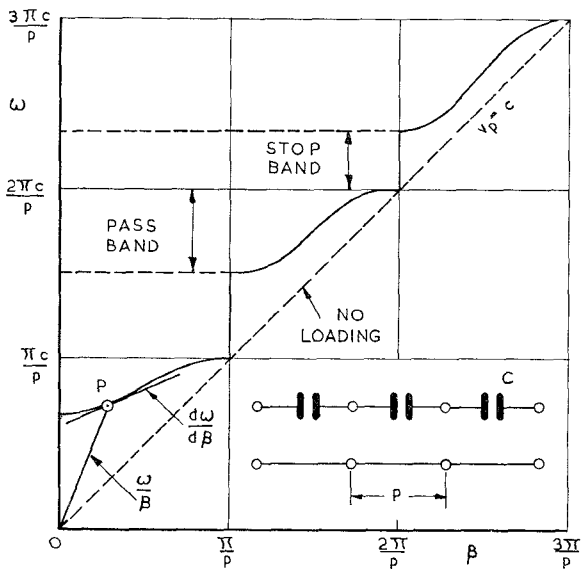

Fig. 3—Frequency characteristic for capacitively loaded line.

$$Z_1 = jZ_{01} \tan (2\pi l/\lambda). \tag{5}$$

The equation of the dispersion curves then becomes

$$\cos \frac{2\pi p}{\lambda_g} = \cos \frac{2\pi p}{\lambda} - \frac{Z_{01}}{2Z_0} \tan \frac{2\pi l}{\lambda} \sin \frac{2\pi p}{\lambda}. \tag{6}$$

The analysis is simplified without affecting the qualitative features if $Z_{01} = 2Z_0$, so that (6) becomes

$$\cos \frac{2\pi p}{\lambda_g} = \left[\cos \frac{2\pi (p+l)}{\lambda} \right] \Big/ \cos \frac{2\pi l}{\lambda} \tag{7}$$

which is plotted in Fig. 4 for $l/p \simeq 1.2$. At low frequencies the loading is inductive, but as ω increases a cutoff occurs when $\lambda_g = 2p$, a standing wave being produced with antinodes at the stubs. The frequency at which this cutoff occurs is less than the lowest or first resonant frequency of the loading reactor. This first resonance occurs when the effective length of the stub is $\frac{1}{4}\lambda$ and the attenuation in the guide is then infinite. From the cutoff frequency to the frequency at which the stub length is $\frac{1}{4}\lambda$, the phase change along one section of the guide remains at the value π.

At the resonant frequency, the loading on the guide changes from inductive to capacitive and the phase difference across a section changes by π. The phase change remains constant at zero until the next pass band is reached. At the beginning of the second pass band, the loading is capacitive with a corresponding frequency characteristic. When the effective length of the stub becomes $\frac{1}{2}\lambda$, it is again resonant with a node of electric field at the mouth of the resonator and $\lambda_g = \lambda$. For a higher frequency, the loading is inductive and a cutoff occurs at a frequency approaching the value for which the resonator length is $\frac{3}{4}\lambda$. The same cycle of events is repeated at all resonant lengths $(m\lambda + \frac{1}{2}\lambda)/2$ where m is a positive integer. At frequencies for which the effective length of the stub is $m\lambda/2$, the loading changes from capacitive to inductive and $\lambda_g = \lambda$.

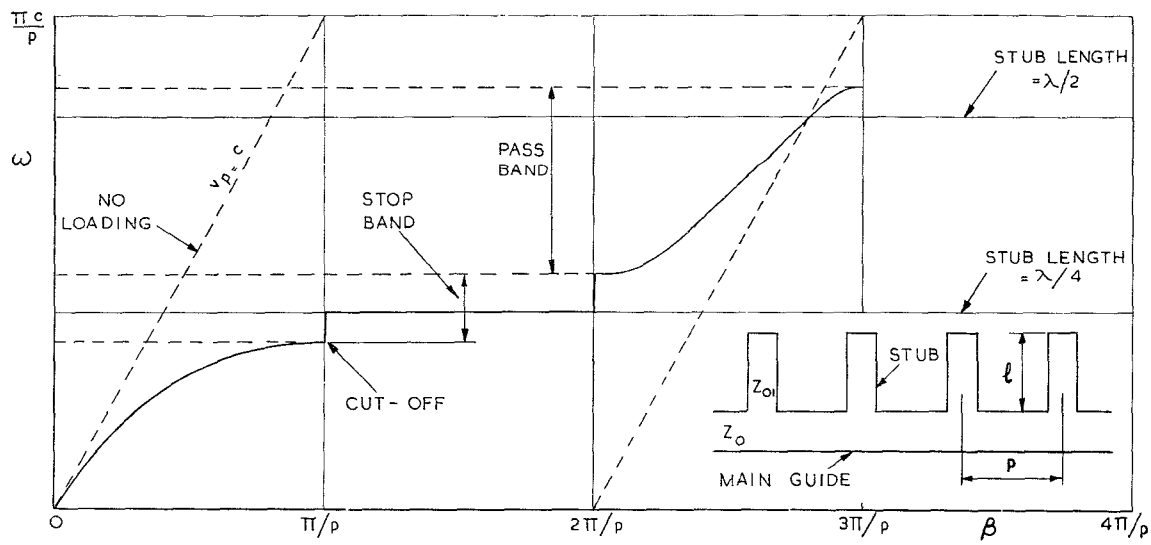

Fig. 4—Frequency characteristic for a parallel-plate line loaded with stubs.

At frequencies such that $\omega = m\pi c/p$, further cutoff values occur. The stop band associated with this type of cutoff is the same as that obtained with inductive or capacitive loading. No resonance occurs in the cavities and the phase change across a section of the guide remains constant throughout the stop band. On both sides of the stop band, the pass bands are either both inductive or both capacitive. In the former case, $\omega = m\pi c/p$ is a low-frequency cutoff for the pass band, and in the latter, it is a high-frequency cutoff. For example, if $l/p = 0.2$, the first stub resonance occurs at $\omega = 2.5\pi c/p$; before this frequency is reached, the dispersion curve shows inductive stop bands at both $\pi c/p$ and $2\pi c/p$.

The phase velocity $v_p = \omega/\beta$ for any point P on the dispersion curve is given by the slope of the line joining the point to the origin. The group velocity $v_g = d\omega/d\beta$ is given by the slope of the curve at the particular point. Provided that the attenuation coefficient is not too great, v_g is also the energy velocity [30] defined as the rate of flow of energy through a cross section of the guide to the energy stored per unit length, the ratio being averaged over one complete section. If Q_u relates to the resonance of the loaded line which is short-circuited at both ends, the attenuation in the pass bands is given in nepers per meter by [233]

$$\alpha = \omega/(v_g Q_u). \tag{8}$$

The dispersion or rate of variation of phase velocity with frequency may determine the useable bandwidth of a periodic structure in a practical device; it is given by

$$dv_p/d\omega = (v_p/\omega)(1 - v_p/v_g). \tag{9}$$

Information about the stop bands is obtained [167] by substituting $\cos(\beta - j\alpha)p$ for $2\pi p/\lambda_g$ in (6). The attenuation in nepers per section αp is then given by

$$\cos(\beta - j\alpha)p = \cos\frac{2\pi p}{\lambda} - \frac{Z_{01}}{2Z_0}\tan\frac{2\pi l}{\lambda}\sin\frac{2\pi p}{\lambda}. \tag{10}$$

The attenuation is zero near the edges and becomes infinite at the center of the resonance stop bands, but remains finite in the inductive and capacitive stop bands. The treatment given for the frequency characteristics has assumed that there is a nearly loss-free system and, moreover, the simple relation of (8) predicts infinite attenuation as the edges of the pass band are approached. These difficulties have been overcome by Butcher [36] who, in taking into account the effect of both conductor and dielectric losses, introduced a complex Q factor which can be used in the pass and stop bands.

Space Harmonics

The frequency characteristics given so far have been for the case when $n = 0$ in (1); that is, only one value of phase velocity has been given explicitly for a particular frequency. The instantaneous potential waveform along the guide is, however, not sinusoidal, but changes discontinuously across the loading impedances and can be described in terms of Fourier analysis as a sum of a series of space harmonics. The amplitudes of these harmonics depend on the form of the potential field which is controlled by the particular structure of the periodic guide. For example, the potential of a travelling wave on a parallel plate line with stubs of aperture b_1, assuming that the electric field strength is constant across the mouth, is given by [167]

$$\sum_n \left[\left(\sin\frac{1}{2}b_1\beta_n\right)\Big/\frac{1}{2}b_1\beta_n\right]e^{j(\omega t - \beta_n z)}. \tag{11}$$

If β_0 is given the value $\pi/4p$, (1) gives

$$\beta_n = (\pi/4p) + (2\pi n/p). \tag{12}$$

The instantaneous waveforms of the harmonics corresponding to $n = -1, 0, +1$ are shown in Fig. 5(a).

The frequency characteristic of a periodic stub loaded structure which includes all space harmonics from $n = -2$ to $n = +3$ is shown by the full lines of Fig. 5(b). It will be seen that the phase velocities of the various harmonics are different and that those for $n = 0, +1, +2$, and $+3$ are positive, while those for $n = -1$ and -2 are negative. At the cutoff frequencies, for every space harmonic with positive phase velocity there is one with an equal and opposite phase velocity. Further investigation shows that the amplitudes of these pairs are also equal and therefore at a cutoff frequency, the guide can support only standing waves. If v_p is the phase velocity at a point A, geometrical considerations show that the phase velocity at corresponding points such as B, C, D, and E is given by $v_p p/(n\lambda_g + p)$.

The group velocities of all the space harmonics are seen to be equal for any given frequency and to have the same direction as that of the energy. For n negative, the phase velocity is always opposite in direction to the group velocity. Such space harmonics are termed reverse or backward waves and, in particular, it is possible to have periodic structures in which the fundamental is itself a reverse wave. The complete characteristic contains a range of upper branches corresponding to resonances of the stubs. Two conventions are in use for the numbering of these branches. In one, the fundamental is taken to be that space harmonic with the highest phase velocity, while in the second, which is adopted here, it is that harmonic which normally has the largest amplitude. In the latter case, with small loading, the characteristic tends to that of the transmission line.

If electromagnetic energy is propagated in both directions, then as shown by the dotted lines of Fig. 5(b), additional curves which represent waves with negative group velocity appear to complete the frequency characteristic. If the forward and backward energies are equal, standing waves are produced not only at the cutoff values but at all frequencies. This analysis may readily be extended from parallel plate lines to waveguides. The characteristic impedance is now given for any one mode of propagation by the ratio of the trans-

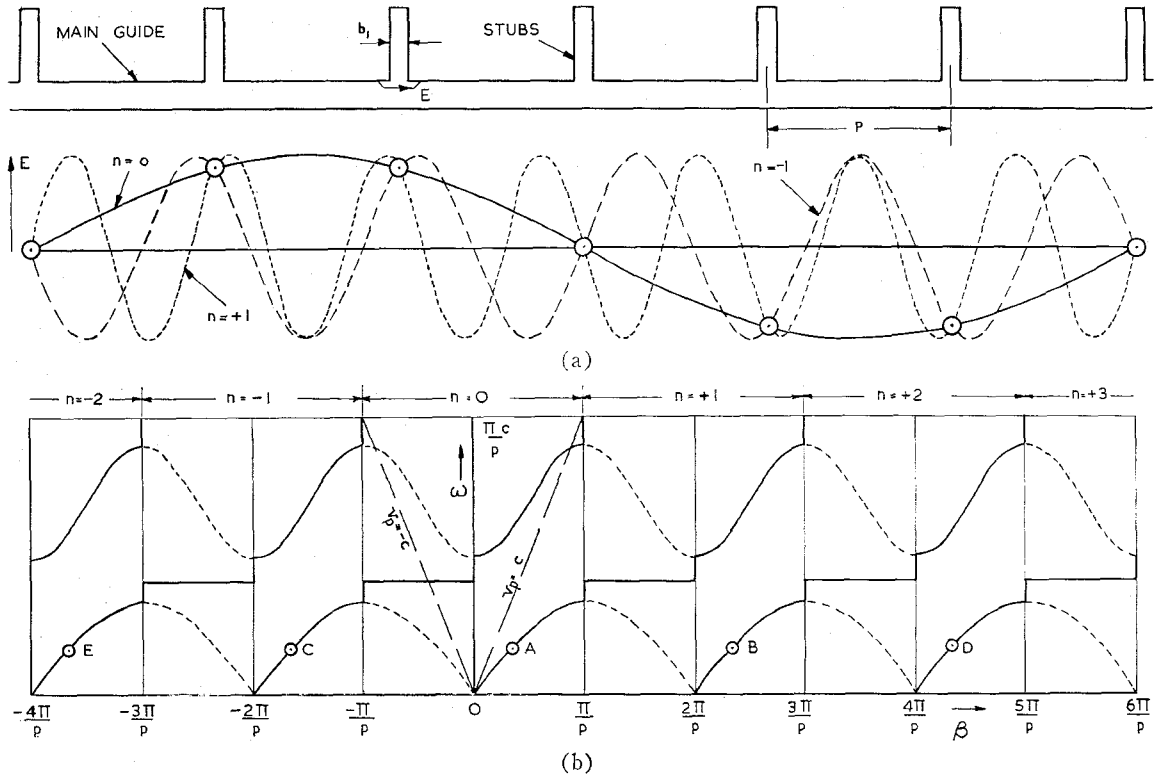

Fig. 5—Forward and backward space harmonics. (a) Stub structure and wave forms of the $n=-1$, 0, and $+1$ space harmonics. (b) Frequency characteristics of the $n=-2$ to $n=+3$ inclusive space harmonics.

verse electric to transverse magnetic field. The frequency characteristics will be similar to those given above except at low frequencies where the guide exhibits a cutoff.

It may be shown [167] that the longitudinal and transverse components of the electric field in the main guide oscillate in quadrature. For capacitive loading where $v_p > c$, the amplitudes vary in the transverse direction according to sine and cosine laws. For inductive loading where $v_p < c$, the transverse propagation constant is real and the amplitudes decay according to hyperbolic sine and cosine laws; these become exponential some distance from the loaded surface.

Multiply-Periodic Loading

Other properties of periodic structures emerge when the loading is systematically uneven [24], [256]. For example, in the structure shown in the inset of Fig. 6, which consists of series stubs of alternate length, it will be evident that the number of degrees of freedom of the system are now doubled and therefore there will be twice the number of branches in the frequency characteristic. Analysis of the equivalent circuit of this double-stub structure gives [167] the equation of the frequency characteristic as

$$\cos(4\pi p/\lambda_g) = \cos(4\pi p/\lambda) - (Z_{01}/2Z_0)\sin(4\pi p/\lambda)[\tan(2\pi l_l/\lambda) + \tan(2\pi l_s/\lambda)] + (Z_{01}^2/2Z_0^2)\sin^2(2\pi p/\lambda)\tan(2\pi l_l/\lambda)\tan(2\pi l_s/\lambda), \quad (13)$$

where $(4\pi p/\lambda_g)$ is the phase change across one complete section of the line (including a long and a short stub).

The frequencies at cutoff for $\beta=0$ and $\beta=\pi/p$ are given by

$$\cos(4\pi p/\lambda_g) = 1. \quad (14)$$

For $Z_{01}=2Z_0$, (13) then gives

$$\omega = \frac{m\pi c}{p}, \quad (15)$$

$$\omega = \frac{m\pi c}{p}\left\{1 + \frac{l_l}{p} + \frac{l_s}{p}\right\}. \quad (16)$$

The values of ω in (15) are the capacitive or inductive cutoff frequencies, being the beginning or end of a stop band. The values of ω in (16) which depend upon l_l and l_s give the cutoff frequencies when adjacent resonators are oscillating in antiphase.

The frequencies at cutoff for $\beta=\pi/2p$ are given by

$$\cos(4\pi p/\lambda_g) = -1, \quad (17)$$

and, for $Z_{01}=2Z_0$, (13) gives

$$\omega = \frac{\pi c}{2}\frac{2m+1}{p+l_l}, \quad (18)$$

$$\omega = \frac{\pi c}{2}\frac{2m+1}{p+l_s}. \quad (19)$$

These values of ω correspond to the occurrence of nodes at the long and short resonators, respectively. If the stubs are all of length l, the frequency for $\beta=\pi/2p$ is given from (7) by

$$\omega = \frac{\pi c}{2}\frac{2m+1}{p+l}. \quad (20)$$

Comparison of (20) with (18) and (19) shows that cutoff values of ω at $\beta=\pi/2p$ for the double-stub structure

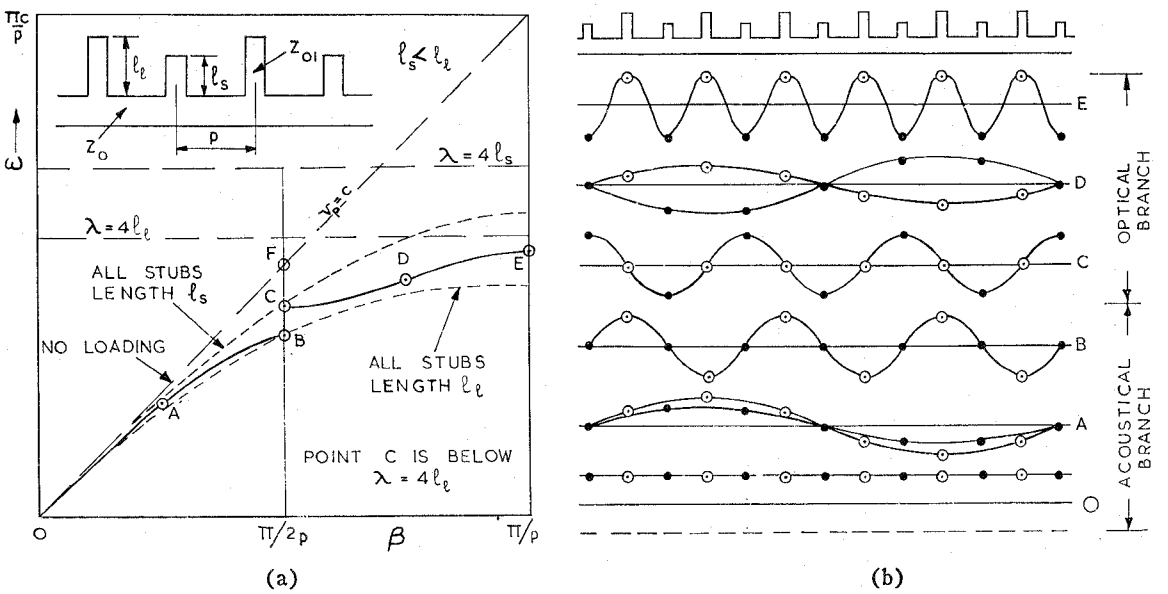

Fig. 6—Inductive double-stub structure. (a) Frequency characteristic. (b) Relative phases of the stubs.

occur at all points where the ordinate $\pi/2p$ cuts the curves of the two uniformly-loaded lines.

Thus the frequency characteristic of the double-stub periodic structure will be similar to that of the simple structure until the phase constant approaches the values at which the cutoffs occur. The characteristics will depart at these points since standing waves can occur with either nodes or antinodes at the modified resonators. These standing waves will have the same wavelength but different frequencies and will be displaced with respect to each other by $\frac{1}{4}\lambda_g$.

The useful properties of this structure occur when the ratio l_l/l_s is not too great, for instance, between 1 and 2. The frequency characteristic may then belong to two classes. In the first class shown in Fig. 6(a), the resonances of the stubs occur at a higher frequency than the two standing waves at B and C when $\beta=\pi/2p$. Therefore, in passing from one branch to the other, the loading remains inductive and there is no change in the phase coefficient at $\beta=\pi/2p$. As Z_{01} is reduced from the value $2Z_0$, the initial portion of the characteristic for all stub lengths tends to follow the $v_p=c$ line more closely and vice versa if Z_{01} is increased; the cutoff frequencies are also modified. From analogy with the characteristics of crystal lattices containing diatomic molecules, the lower curve is sometimes termed the acoustical branch and, as shown in Fig. 6(b), the phase of the oscillations in the resonators differs by less than $\frac{1}{2}\pi$ and tends to zero when β approaches zero. The upper curve is termed the optical branch and the phase of the neighbouring resonators differs by more than $\frac{1}{2}\pi$ and approaches π as β approaches π/p.

In the second class illustrated by Fig. 7, a resonance of the larger stub occurs between the two standing waves at $\beta=\pi/2p$ when $l_l=\frac{1}{4}\lambda$ and results in a change from inductive to capacitive loading. The loading remains capacitive until a frequency is reached where $\lambda_g=\lambda$; *i.e.*, the phase velocity is equal to the free-space

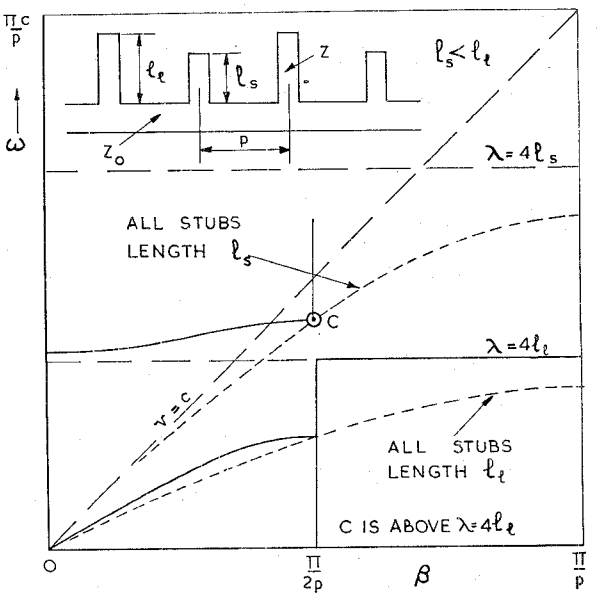

Fig. 7—Resonant double-stub structure.

velocity. At this frequency the capacitance of the small resonator and inductance of the larger resonator may be regarded approximately as a series resonant circuit. At a still higher frequency the loading is again inductive. For periodic structures with more than two lengths of stubs, the number of branches in the frequency characteristic will equal the number of different lengths of resonator; *i.e.*, the number of frequencies corresponding to a given phase constant is equal to the number of degrees of freedom associated with each section of the line. For example, in a structure in which there are three stubs per section and every third is modified, one of the many possible characteristics takes the form shown in Fig. 8. It has been shown [167] that under certain conditions and over a limited frequency range, the dispersion is small since the phase velocity is nearly constant.

Dielectric-Clad Metal Structures

Plane Waves Over Flat Surfaces

In conventional transmission systems, at microwave frequencies the electromagnetic energy is effectively confined to a closed region of space by means of conducting walls. Under certain conditions other types of transmission may exist in which the energy is not rigidly confined but rather is bound to a surface or structure. Such a guiding structure can support [32] three classes of waves: first, a continuous spectrum of propagating waves and second, a continuous spectrum of evanescent waves which are exponentially attenuated in the direction of propagation. The third class represents one or more surface waves which, by careful launching, can be made to predominate.

These surface waves [20], [190], [292], [293] are forms of electromagnetic energy which propagate without radiation along an interface between two media with different physical properties. The electromagnetic field extends to infinity in the transverse direction but the energy density decreases with distance so that, in practice, most of the energy of the wave is constrained to flow in the immediate neighborhood of the structure. The only flow of energy away from the interface is that required to supply the losses in the media concerned. The properties of these waves are governed by the surface impedance Z_s defined as the ratio of the tangential components of the electric and magnetic field vectors. In general, Z_s is complex, having both resistive and reactive components.

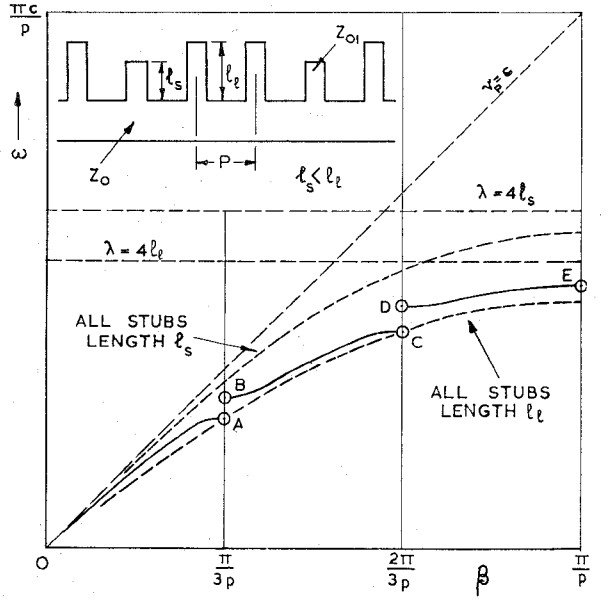

Fig. 8—Triple-stub multiply-periodic structure.

To comply with the conditions required for the support of surface waves, the interface must be straight in the direction of propagation of the wave but, transversely, it can take a variety of shapes and forms. The external medium is usually air, while the structure may consist of dielectric, either alone or in combination with a conductor, and metal surfaces provided with periodic corrugations. For example, a wave which travels without change of pattern over a flat surface bounding [6] two homogeneous media of different conductivity and permittivity was shown by Zenneck [291] to be a particular solution of Maxwell's equations. Such a wave is characterized [93] by the presence of a longitudinal component of the electric field vector; it is a TM wave.

Surface waves can be propagated [44], [239], [257] in plane or radial form over a dielectric-clad flat structure and in axial form along a cylinder. Such waves can also be supported by conical guides and, in particular, there are surface waves of various forms in between the axial and the radial variety. A typical flat surface is shown in Fig. 9(a) in which medium (m) is a metallic conductor, (d) is a dielectric slab, and (a) is air. For the dominant TM_0 plane wave travelling in the z direction with propagation coefficient γ, the three components of field required to satisfy the wave equation in the metal are given by Barlow and Cullen [15] as

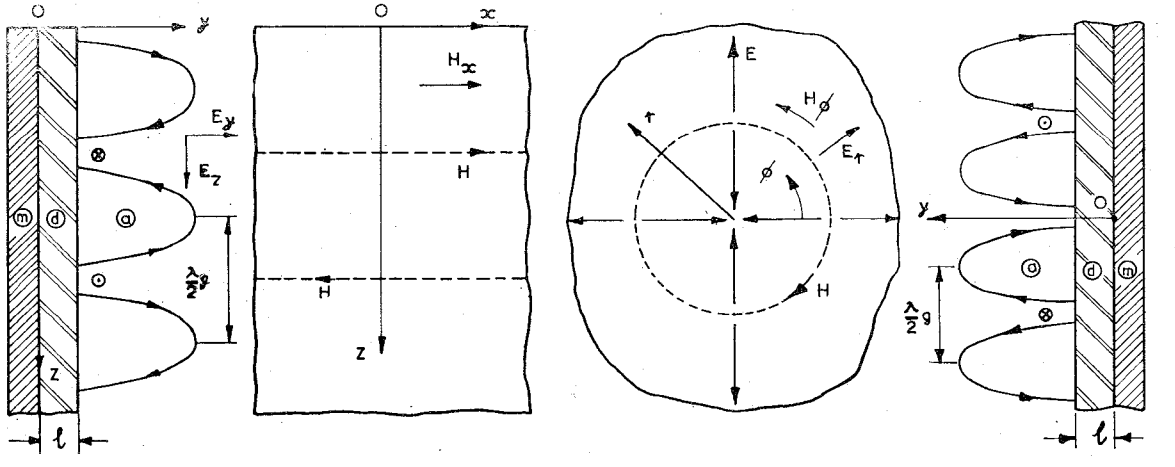

Fig. 9—Propagation over flat dielectric-clad surfaces. (a) Plane wave. (b) Radial wave. The properties of the media are (m) Metal, $\mu_m = \mu_0$, $\epsilon_m\epsilon_0$, σ_m, (d) Dielectric, $\mu_d = \mu_0$, $\epsilon_d\epsilon_0$, $\sigma_d = 0$, and (a) Air, $\mu_a = \mu_0$, $\epsilon_a\epsilon_0$, $\sigma_a = 0$.

$$H_{xm} = Ae^{u_m y}, \tag{21}$$

$$E_{zm} = A\left(\frac{u_m}{\sigma_m + j\omega\epsilon_m\epsilon_0}\right)e^{u_m y}, \tag{22}$$

$$E_{ym} = A\left(\frac{\Gamma}{\sigma_m + j\omega\epsilon_m\epsilon_0}\right)e^{u_m y}. \tag{23}$$

The factor $e^{(j\omega t-\gamma z)}$ is omitted for convenience and A is a constant. The propagation coefficient along the y-axis,

$$u_m = a_m + jb_m, \tag{24}$$

represents an attenuation a_m and phase change b_m for a wave travelling inwards from the surface where $y \leq 0$. Within this medium

$$\gamma^2 + u_m^2 = j\omega u_0(\sigma_m + j\omega\epsilon_m\epsilon_0). \tag{25}$$

In the external air medium the fields for $y \geq l$ are similarly given by

$$H_{xa} = Ae^{-u_a y}, \tag{26}$$

$$E_{za} = -A(u_a/j\omega\epsilon_0)e^{-u_a y}, \tag{27}$$

$$E_{ya} = A(\gamma/j\omega\epsilon_0)e^{-u_a y}. \tag{28}$$

Here

$$u_a = a_a - jb_a \tag{29}$$

because the field not only decays at the rate a_a with increasing transverse distance but also suffers a progressive phase change b_a for a wave travelling towards the surface. In this medium the propagation coefficients satisfy

$$\gamma^2 + u_a^2 = -\omega^2/c^2. \tag{30}$$

Within the solid dielectric there exists a standing wave whose magnetic field is given by

$$H_{xd} = A_d' \cosh u_d y + A_d'' \sinh u_d y \tag{31}$$

and in this medium

$$\gamma^2 + u_d^2 = -\epsilon_d\omega^2/c^2. \tag{32}$$

The conditions for matching the field components at the boundaries between the different layers yields

$$\tanh u_d l = -\left[\frac{1 + \left(\frac{j\omega\epsilon_d\epsilon_0}{\sigma_m + j\omega\epsilon_m\epsilon_0}\right)\left(\frac{u_m}{u_a\epsilon_d}\right)}{\frac{u_d}{u_a\epsilon_d} + \left(\frac{j\omega\epsilon_d\epsilon_0}{\sigma_m + j\omega\epsilon_m\epsilon_0}\right)\left(\frac{u_m}{u_d}\right)}\right]. \tag{33}$$

The impedance looking into the surface of the solid dielectric is

$$Z_s = R_s + jX_s = E_{za}/H_{xa} = -u_a/j\omega\epsilon_0. \tag{34}$$

In the case of a good conductor, the surface impedance has nearly equal real and imaginary parts and is given by

$$Z_m = R_m + jX_m = (1 + j)(\omega\mu_0/2\sigma_m)^{1/2}. \tag{35}$$

The total surface resistance in the case of loss in the dielectric is given by

$$R_s = R_m + R_d = R_m + (\beta_w l/\epsilon_d Z_w)\tan\delta. \tag{36}$$

This resistance therefore depends upon the conductivity of the metal if the dielectric is loss free. The surface reactance X_s is made up of one component arising from the metal and another,

$$X_d = \omega\mu_0 l(\epsilon_d - 1)/\epsilon_d, \tag{37}$$

for which the layer of solid dielectric is responsible. These two components are of the same order of magnitude when the thickness of the dielectric is about equal to the skin depth δ_s of the metal.

If l is assumed to be small so that $\tanh u_d l \simeq u_d l$ and $u_d l \ll 1$, (33) gives

$$u_a = a_a - jb_a = j\beta_w Z_s/Z_w. \tag{38}$$

In general, the higher the surface reactance and the higher the frequency, the greater the decay factor a_a so that the field becomes concentrated more closely in the immediate vicinity of the surface. Any increase of R_s increases the inclination of the wavefront at the surface, measured from the normal and this, in turn, increases the phase velocity along the interface. On the other hand, it may be anticipated by analogy with electric circuits that the corresponding phase velocity would be reduced by an inductive surface reactance and increased by a capacitive one.

In order to obtain the attenuation and phase-change coefficients along the surface in the direction of propagation, (29) and (30) are substituted in the expression for γ to give [137]

$$\alpha = \beta_w R_s X_s/Z_w^2, \tag{39}$$

$$\beta = \beta_w\left\{1 - \frac{1}{2}\left(\frac{R_s^2 - X_s^2}{Z_w^2}\right)\right\}. \tag{40}$$

If $\beta \simeq \beta_w$, the velocity of propagation becomes

$$v_p = c\left\{1 + \frac{1}{2}\left(\frac{R_s^2 - X_s^2}{Z_w^2}\right)\right\}. \tag{41}$$

Eq. (39) shows that α is proportional to R_s and X_s while (41) shows that $v_p > c$ if R_s is substantially greater than X_s, and vice versa. Values of loss and phase velocity have been calculated [12] for frequencies of 0.3–30 kmc for a dielectric with $\epsilon_d = 4$, $\tan\delta = 0.001$, and thicknesses of 0.1–10 mm. At 10 kmc a layer 0.5 mm thick gave a loss of 10^{-3} db/m and a phase velocity of 0.65 c.

Radial Waves Over Flat Surfaces

The geometry and field pattern of a wave propagating radially over a flat dielectric-clad metal surface are shown in Fig. 9(b). The field components in the metal, omitting the time factor $e^{j\omega t}$, are [15]

$$H_{\phi m} = Ae^{u_m y}H_1^{(2)}(-j\gamma r), \tag{42}$$

$$E_{rm} = -A\left(\frac{u_m}{\sigma_m + j\omega\epsilon_m\epsilon_0}\right)e^{u_m y}H_1^{(2)}(-j\gamma r), \quad (43)$$

$$E_{ym} = A\left(\frac{j\gamma}{\sigma_m + j\omega\epsilon_m\epsilon_0}\right)e^{u_m y}H_0^{(2)}(-j\gamma r), \quad (44)$$

with (24) and (25) as previously. In the external air medium,

$$H_{\phi a} = Ae^{-u_a y}H_1^{(2)}(-j\gamma r), \quad (45)$$

$$E_{ra} = A(u_a/j\omega\epsilon_0)e^{-u_a y}H_1^{(2)}(-j\gamma r), \quad (46)$$

$$E_{ya} = A(\gamma/\epsilon_0)e^{-u_a y}H_0^{(2)}(-j\gamma r) \quad (47)$$

with (29) and (30) as previously.

By comparing (21)–(23) and (42)–(44) or (26)–(28) and (45)–(47), it will be seen that the radial form of the modified Zenneck wave has the same field distribution in the y direction as the corresponding plane wave. Along the radial coordinate r, the wave propagates according to the Hankel function and, at large distances, the amplitude follows an exponential of the form $e^{-\gamma r}/r^{\frac{1}{2}}$.

There is again a standing wave in the intervening medium and the surface impedance looking into the dielectric-clad metal is given by

$$Z_s = R_s + jX_s = -E_{ra}/H_{\phi a}. \quad (48)$$

The values of R_s, X_s as well as the attenuation and phase-change coefficients, are the same as for the plane wave.

Axial Cylindrical Waves

It was theoretically shown by Sommerfeld [244] that a straight cylindrical conductor of finite conductivity and having a smooth surface can act as a guide for electromagnetic waves. This surface wave propagation was shown to take place for infinite conductivity by Harms [109] provided that the surface of the metal is coated with a dielectric layer. Although higher-order modes are associated [13], [116] with this guide, attention is usually focused on the dominant TM_{00} mode. The geometry and field distribution of this wave are shown in Fig. 10; when the radius of the cylinder is increased to infinity, this axial wave becomes identical with the plane wave over a flat surface. Following the work of Goubau [94] the dielectric-coated wire has been extensively examined [22], [42], [54], [55], [58], [72], [89], [131], [133], [134], [136], [157], [210], [224] as a transmission line for microwave frequencies.

For propagation along the z-axis, the field components inside the metal, omitting the term $e^{(j\omega t-\gamma z)}$, are given by [15]

$$H_{\theta m} = A\left(\frac{\sigma_m + j\omega\epsilon_m\epsilon_0}{ju_m}\right)J_1(ju_m r), \quad (49)$$

$$E_{zm} = AJ_0(ju_m r), \quad (50)$$

$$E_{rm} = A(\gamma/ju_m)J_1(ju_m r), \quad (51)$$

with (24) and (25) for the flat surface. In the external air medium,

$$H_{\theta a} = A(\omega\epsilon_0/u_a)H_1^{(1)}(ju_a r), \quad (52)$$

$$E_{za} = AH_0^{(1)}(ju_a r), \quad (53)$$

$$E_{ra} = A(\gamma/ju_a)H_1^{(1)}(ju_a r), \quad (54)$$

with (29) and (30) as for the flat surface. The argument of the Hankel functions is imaginary and thus the external fields decay at a rate which becomes exponential for large radii.

The surface impedance looking into the dielectric sheath, with $r = r_1$, is

$$Z_s = R_s + jX_s = \frac{E_{za}}{H_{\theta a}} = \left(\frac{u_a}{\omega\epsilon_0}\right)\left[\frac{H_0^{(1)}(ju_a r_1)}{H_1^{(1)}(ju_a r_1)}\right] \quad (55)$$

which, when $r_1 \to \infty$, becomes $j(u_a/\omega\epsilon_0)$, the value for the flat surface given in (34). For cylinders of small diameter, the curvature of the equiphase surfaces near the wire has an important effect on the wave impedance which may change from being inductive at a great dis-

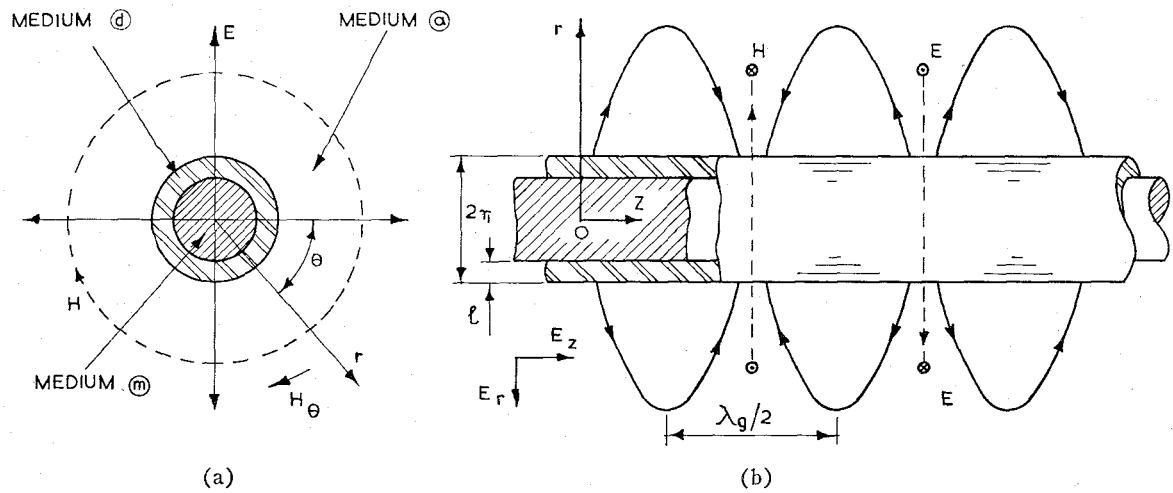

Fig. 10—Axial propagation on a dielectric-clad cylinder. The properties of the media are (m) Metal, $\mu_m = \mu_0$, $\epsilon_m\epsilon_0$, σ_m, (d) Dielectric, $\mu_d = \mu_0$, $\epsilon_d\epsilon_0$, $\sigma_d = 0$, and (a) Air, $\mu_a = \mu_0$, $\epsilon_a\epsilon_0 = \epsilon_0$, $\sigma_a = 0$.

tance from the wire to being capacitive near the wire. In fact, a bare copper wire which has a very small inductive component of impedance at its surface is a practical guide for the Sommerfeld surface wave at microwave frequencies.

Experiments on dielectric-coated wires have been reported at microwave frequencies [92], [95], [98], [211] including 3 kmc [99], 10 kmc [45], [145] and at ultra-high frequencies [198], [231]. The properties of the lines are found to agree closely with those predicted by theory. As an example [97], Fig. 11(a) shows the radius r_2 at which the field is 90 per cent of its maximum, the reduction $\delta v_p/v_p$ of phase velocity and the fraction $\delta W/W$ of the energy propagated in the dielectric layer, all as functions of the thickness of the layer. The wire radius was assumed to be 0.1 cm and the frequency was 3 kmc. The attenuation for wires coated with enamel, $\epsilon=3$, $\tan\delta=0.008$ is given in Fig. 11(b). A conductor for 35 kmc need only be 0.056-inch diameter with a thin coating of enamel.

Miscellaneous Surface Circuits

Transverse Corrugations

The surface reactance of a guide may be enhanced by coating it with an artificial dielectric such as a corrugated structure [27], [76], [121]. The flat surface shown in Fig. 12(a) was first examined by Cutler [64] who considered the corrugations as short-circuited parallel-plate stubs with an impedance given by (5). Assuming that the surface has infinite conductivity and omitting the factor $e^{j(\omega t-\beta z)}$, the field components in the air medium outside the grooves are given by

$$H_{xa} = jA(\beta_w/u_a Z_w)e^{-u_a y}, \tag{56}$$

$$E_{za} = Ae^{-u_a y}, \tag{57}$$

$$E_{ya} = -jA(\beta/u_a)e^{-u_a y}, \tag{58}$$

and (30) becomes

$$\beta^2 - u_a^2 = \beta_w^2 = \omega^2/c^2. \tag{59}$$

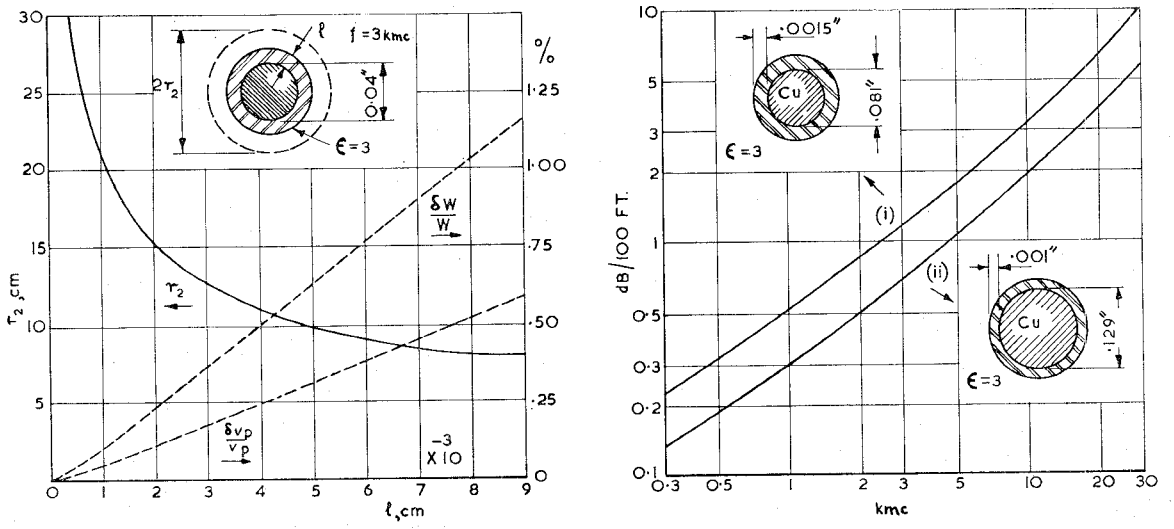

(a) (b)

Fig. 11—Properties of a dielectric coated wire. (a) 90 per cent field radius, change in phase velocity and propagation of energy stored in the dielectric. (b) Attenuation for two sizes of enamelled wire.

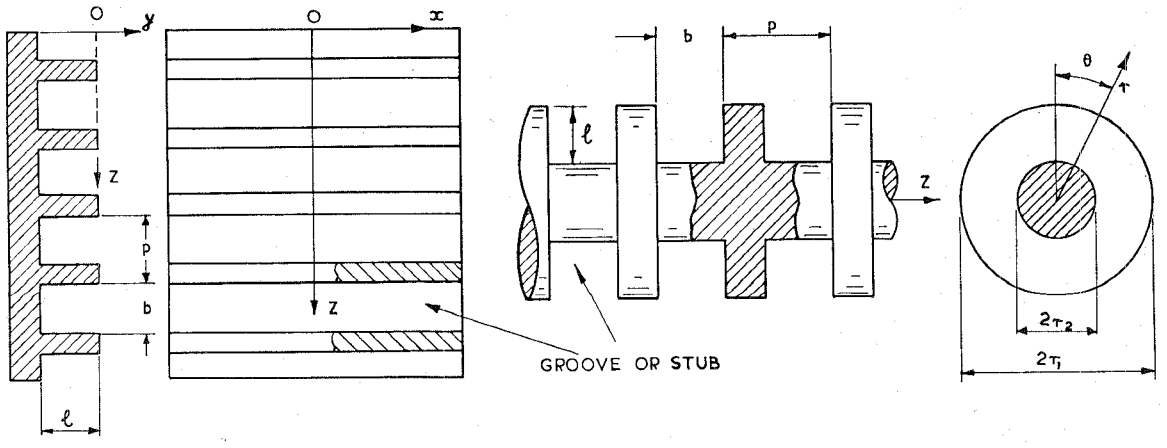

(a) (b)

Fig. 12—Propagation along corrugated surfaces. (a) Plane with parallel grooves. (b) Cylindrical with radial grooves.

The wave is a TM type since the magnetic field lies totally within the transverse plane.

Since the structure is periodic, the wave travelling along the surface consists of a fundamental plus space harmonics whose relative amplitudes are functions of stub width, length, and pitch. The surface impedance of the surface between the corrugations is zero, since E_{za} vanishes there. If the width of the stub is small compared with the guide wavelength, the surface impedance can be given its average value,

$$Z_s = -jZ_w(b/p) \tan (2\pi l/\lambda). \tag{60}$$

Matching this to the uniform surface impedance given by E_{za}/H_{xa} gives

$$u_a = \beta_w(b/p) \tan (2\pi l/\lambda). \tag{61}$$

This relation shows that propagation is possible in certain bands where u_a is positive, whereas, for other regions, u_a is negative and waves cannot be propagated. In the first pass band as l increases from 0 to $\frac{1}{4}\lambda$, the surface impedance is inductive and increases from zero to infinity. Moreover, the phase velocity varies from c to zero while the field intensity as a function of distance from the surface changes from a small to a large exponential decrease. Such results have been confirmed [213] by experiments on flat corrugated surfaces.

In the case of the corrugated cylinder in Fig. 12(b) the surface-wave field has components given by

$$E_{za} = AH_0^{(1)}(ju_a r), \tag{62}$$

$$E_{ra} = A(\beta/u_a)H_1^{(1)}(ju_a r), \tag{63}$$

$$H_{\theta a} = A(\beta_w/u_a Z_w)H_1^{(1)}(ju_a r), \tag{64}$$

with (59) as previously. If the dimensions are such that the field is caused by the principal wave only, the guide behaves as if it had a uniformly distributed surface impedance given by

$$Z_s = \frac{E_{za}}{H_{\theta a}} = \frac{u_a Z_w}{\beta_w} \frac{H_0^{(1)}(iu_a r)}{H_1^{(1)}(ju_a r)}. \tag{65}$$

The TEM wave impedance presented by the individual stub elements is given by [140]

$$Z_1 = -jZ_w \frac{Y_0(\beta_w r_2)J_0(\beta_w r_1) - J_0(\beta_w r_2)Y_0(\beta_w r_1)}{Y_0(\beta_w r_2)J_1(\beta_w r_1) - J_0(\beta_w r_2)Y_1(\beta_w r_1)}. \tag{66}$$

Here, again, a first-order approximation for the surface impedance includes a factor (b/p), but a more accurate empirical result,

$$Z_s = (b/p)Z_1(1 - \tfrac{1}{2}e^{-l/b} - \tfrac{1}{2}e^{-5l/b}), \tag{67}$$

is applicable for all values of surface parameters provided that $p < \frac{1}{4}\lambda$. The theoretical relations for the surface reactance have been supported by experiments of Barlow and Karbowiak [17] at 2.35 kmc and 9.4 kmc using resonant lines about 4 feet in length. The reactance as a function of stub width is shown in Fig. 13(a) while Fig. 13(b) shows the effect of varying either the length or pitch of the stubs.

Effect of Curvature

If the surface-wave structure is curved in the direction of propagation, radiation takes place. This phenomenon can be qualitatively examined [15], [20] by considering the adjacent equiphase planes between which the field is normally evanescent. On bending the structure, the planes diverge so that the spacing eventually becomes sufficient for them when considered as waveguides to allow propagation and hence radiation of energy. It may be visualized that increase of curvature would increase the radiation while enhancement of the surface reactance would, by confining the field more closely, reduce the radiation. This conception has been employed [19] to calculate the power radiated from a curved surface.

These azimuthal surface waves may be analyzed by finding [77], [117], [178] a solution of Maxwell's equations which represents their propagation. For a dielectric sheet, as in the inset of Fig. 14(a), bounded on the inside by a perfect conductor, the fields at a point r, θ, z may be constructed from cylindrical wave functions. Assuming that there is TM mode propagation and a dielectric constant of 4.0, the dotted lines in Fig. 14(a) give the dielectric thickness for various radii of bending. It will be observed that as the cylinder radius is decreased, a thicker dielectric film is required to maintain the same degree of trapping of the wave. However, for radii greater than a few wavelengths, the required film thickness is a slowly changing function of radius which smoothly approaches the plane value. An analysis for TE waves yields the full lines of Fig. 14(a) and, here again, many of the same considerations apply. A corrugated surface is shown in Fig. 14(b) where θ_p, θ_b are the angular stub pitch and width, respectively. The curves plotted again show that for radii of curvature exceeding several wavelengths, the value of λ/λ_g is almost independent of radius but depends chiefly on the corrugation geometry.

Launching and Other Devices

The important practical aspect of the efficient launching of surface waves may be ensured [162] by matching their field pattern with that of the launching device as closely as possible. The exponential decay of the fields above a plane surface does not approximate closely to the constant or sinusoidal distribution inside waveguides and parallel plate lines and the launching of a pure surface wave presents some difficulty. In an unpublished work, G. G. Macfarlane calculated that the range of the surface wave from a finite aperture h is restricted to a distance $h \csc \theta_0$ where θ_0 is the Brewster angle of the material. For a lossless dielectric coated surface, θ_0 is purely imaginary and the range is then infinite. Not all the energy goes into the surface wave because the finite aperture leads [15], [61] to an outward

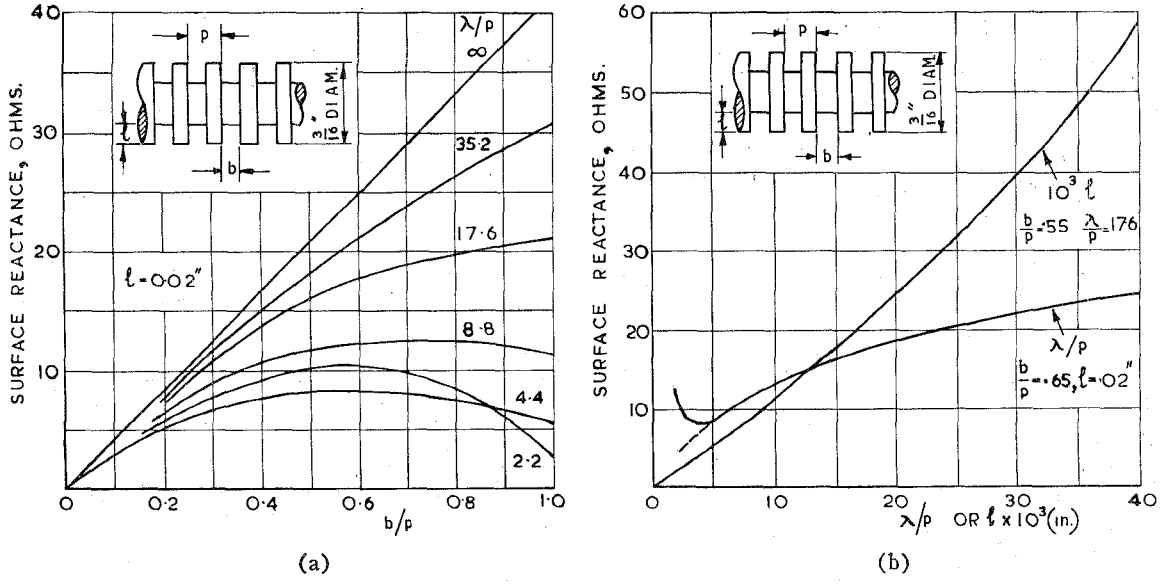

Fig. 13—Properties of a corrugated cylindrical surface. (a) Surface reactance vs groove width. (b) Surface reactance vs groove depth and number per wavelength.

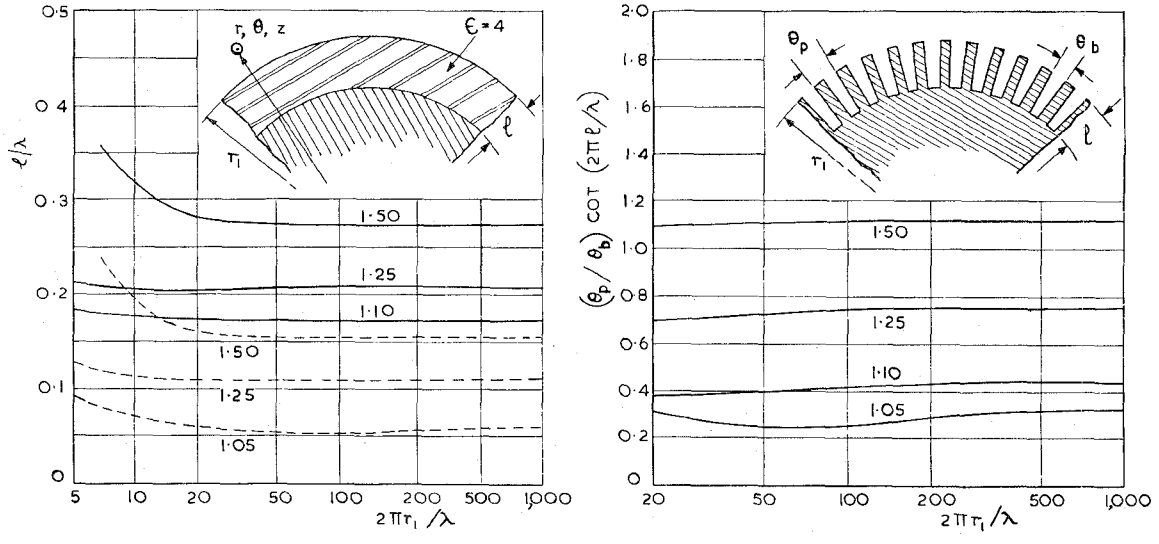

Fig. 14—Azimuthal waves on curved guiding surfaces. (a) Dielectric-clad metal, with TM (dotted line) and TE (full line) modes. (b) Corrugated surface, TM modes. The parameter marked on each curve is λ/λ_g.

travelling radiation wave which represents a loss of energy. The launching efficiency [143] is defined as the power in the desired mode divided by that supplied to the launcher.

The optimum conditions for launching surface waves over a flat structure have been extensively studied [87], [96], [168], [273]. In a typical theoretical and experimental investigation, Rich [208] employed the arrangement shown in Fig. 15 in which a 6-foot×1-foot brass sheet is coated with $\frac{1}{16}$-inch polystyrene. The frequency was 9.5 kmc and the vertical aperture of the flare could be restricted to various heights by a nonreflecting absorbing sheet. The efficiency of the launcher can be determined by first matching it to the surface when terminated by a resistive load. The latter is then replaced by a short circuit and the VSWR measured again; the launching efficiency is then equal to the voltage reflection coefficient. With aperture height of 1, 2, and 3 cm the efficiencies measured were respectively 30 per cent, 60 per cent, and 85 per cent, while from 5 cm, the efficiency flattened out to approach nearly 100 per cent asymptotically. Such results agree very closely with the theoretical values. A practical launcher [213] for a wave along a corrugated surface is shown in Fig. 16(a); two such devices, one for the input and the other for the output, give a power transmission ratio of 0.7.

The launching of a radial surface wave over a flat structure has also been the subject of investigation [28], [29]. In one series of experiments [81] the surface took the form of a large aluminium disk, 5-foot, 6-inch diameter and $\frac{3}{8}$-inch thick; it was electrically loaded to enhance its reactance by either a dielectric sheet or circumferential grooves. Radial slots were provided in the surface to enable probe measurements of field

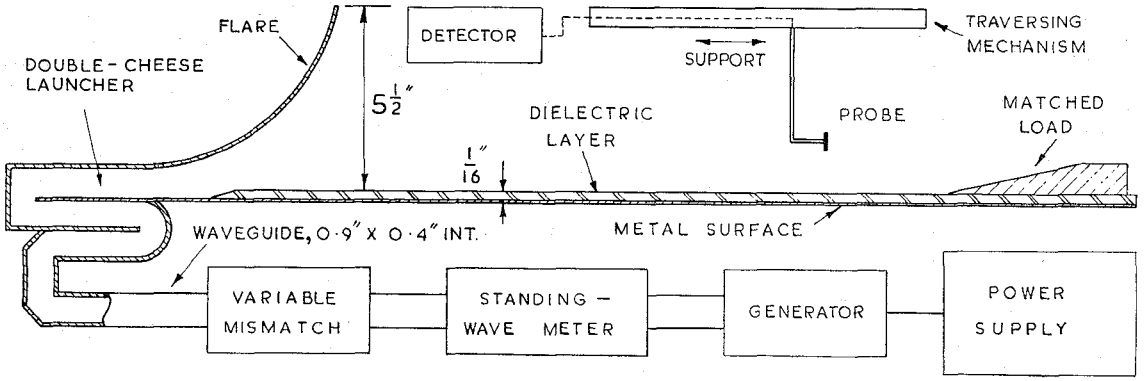

Fig. 15—Launching of waves over a dielectric surface. Frequency, 9 kmc; width of surface, 12 inches; dielectric-polystyrene, $\epsilon = 2.5$.

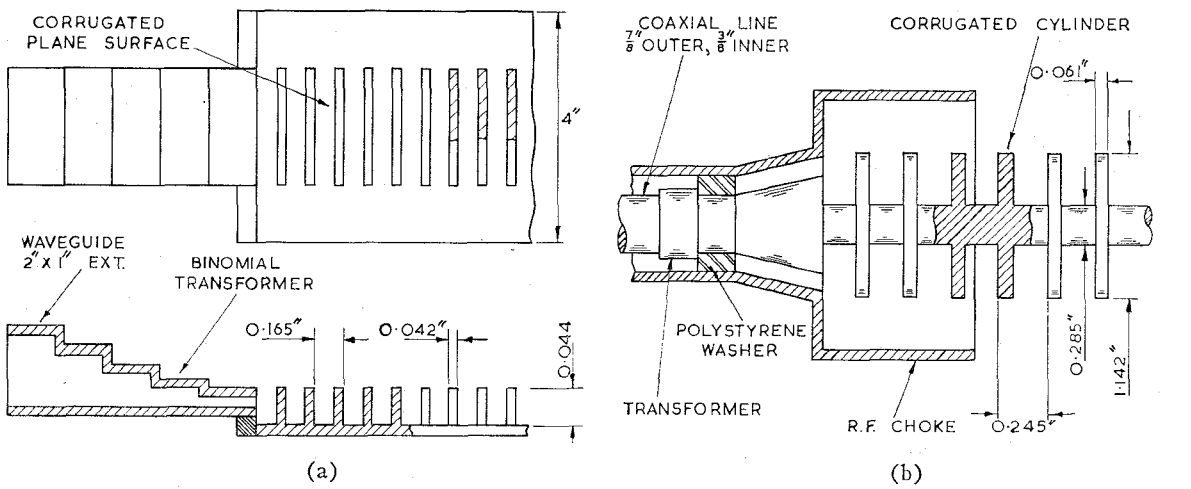

Fig. 16—Launching of waves over a corrugated surface. (a) Plane surface, frequency 5 kmc. (b) Cylindrical surface, frequency 3 kmc.

strength to be made. The launching was via a vertical dipole whose height above the surface was adjustable. At a frequency of 9.5 kmc, the launching efficiencies were as high as 80 per cent for a particular height of the dipole. Slot excitation has been shown [62] to be convenient, and efficient and the use of a circumferential slot in a conducting cylinder leads to symmetry of launching. In one arrangement [33] for 9.5 kmc, the slot is at the circumference of a radial line fed by a coaxial line within the cylinder.

Launching on a cylindrical-surface structure is facilitated because the Hankel function distribution of the radial field intensity approximates to the inverse radius law obeyed by fields inside a coaxial line. The wave is therefore usually [18], [74] launched by flaring the outer conductor of a coaxial line into a cone and continuing the inner conductor to form the transmission line. An alternative is to employ a tapered tube of solid dielectric slipped over the guide but, in either case, the surface wave tends to be contaminated by radiation from the launching device. As an example [213], Fig. 16(b) shows a corrugated cylinder fed from a rigid coaxial line; a typical value of launching efficiency is 90 per cent.

Practical data have been given [262] on surface-wave circuits and many instruments and components have been constructed. Simple corners can be made by employing [41] a large reflecting sheet situated at the intersection of the axes of the mating guides. Similar reflectors have been used to form surface-wave resonators. In one example [14], [16] for 9 kmc the short-circuited ends took the form of flat metal plates about 4-foot diameter and mounted at right angles to the guide. The energy was fed into the resonator by a small annular opening adjoining the guide at one end as shown in Fig. 17(a); the observed surface wave was very pure and thus measurement techniques are facilitated. It may be shown from (40) that

$$\frac{\lambda}{\lambda_g} \simeq 1 - \frac{1}{2}\left[\left(\frac{\lambda}{2\pi}\right)^2 (b^2 - a^2) + \left(\frac{\lambda}{2\pi}\right)^4 a^2 b^2\right] \qquad (68)$$

and, since the length of the circuit at resonance is an integral number of half-wavelengths, the velocity of propagation can be determined. The radial variation of the tangential magnetic field can be measured by a loop probe in the far end-plate of the resonator.

Neighbouring surface-wave lines can interact [173], [174] and thus impedances can be measured by re-

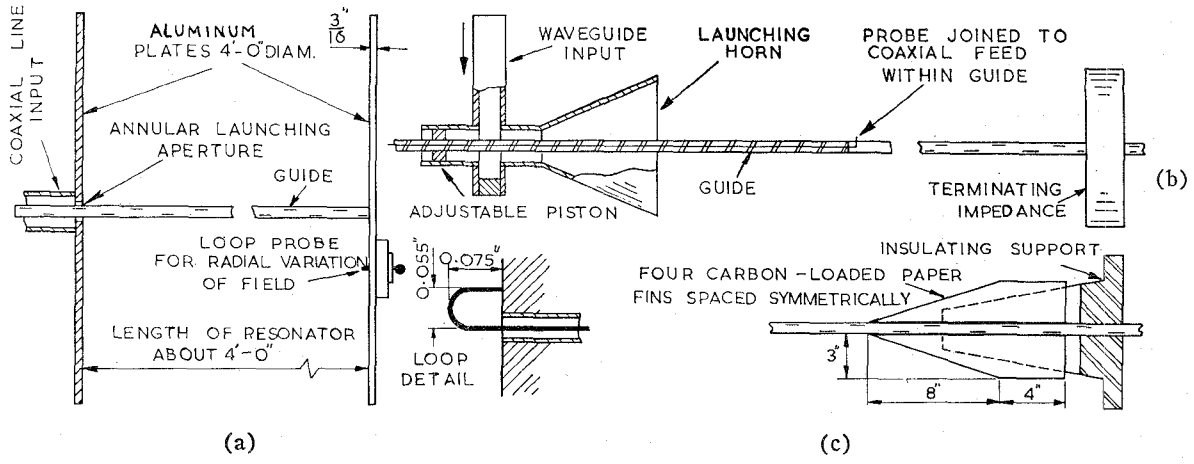

Fig. 17—Measuring apparatus for waves on cylindrical surfaces. Surface-wave resonator with loop detail. (b) Standing-wave meter for surface waves. (c) Matched termination, VSWR = 1.02.

flectometer techniques [226]. The loss of a surface-wave structure can also be measured [219] while the reflection-coefficient of a discontinuity can be determined by the Deschamps method [230]. Greater versatility is achieved by a standing-wave meter constructed in the surface-wave line itself and a typical example [16] is shown in Fig. 17(b). The surface waveguide consists of a metal tube through whose wall the probe projects slightly into the surrounding field. The energy extracted by the probe is taken to the detector via a coaxial line formed by an insulated wire drawn through the tubular guide. The probe projection is fixed and the whole guide with the probe is moveable while the field pattern remains stationary. A suitable matched termination is shown in Fig. 17(c).

Waves on Dielectric Lines

Plane Slabs

The waves considered so far have been TM modes propagating along a surface. In the case of a thick dielectric slab, higher modes may propagate and, depending upon the cross-sectional area of the guide, the proportion of energy flowing in the dielectric or in the external medium can be controlled. One such practical structure, the H-guide [255], consists of a dielectric slab between two parallel conducting strips. Provided that the dielectric has low loss, the attenuation of such a guide is not only less than that of the corresponding rectangular guide but decreases as the frequency increases.

Propagation of energy inside dielectric sheets [263] may be examined [220], [248], [288] by the use of Maxwell's equations, but an analysis depending on the breaking up of the wave into two criss-crossing components leads directly to the cutoff frequencies. Guidance takes place provided that these components are totally reflected at the dielectric/air interface. From Fig. 18(a), this means that the angle of incidence must be greater than the critical angle $\sin^{-1}\epsilon^{-1/2}$; that is,

$$\lambda/\lambda_g = \epsilon^{1/2} \sin \theta. \tag{69}$$

The wave impedance in the z direction is given for TE waves by

$$Z_{TE} = E_y/H_x = Z_w\epsilon^{-1/2}/\sin \theta, \tag{70}$$

and for TM waves by

$$Z_{TM} = E_x/H_y = Z_w\epsilon^{-1/2} \sin \theta. \tag{71}$$

The reflection coefficient for the transverse field component which is parallel to the interface is

$$\rho_{TE} = \frac{\epsilon^{1/2} \cos \theta + j(\epsilon \sin^2 \theta - 1)^{1/2}}{\epsilon^{1/2} \cos \theta - j(\epsilon \sin^2 \theta - 1)^{1/2}} \tag{72}$$

for the E_y component of TE waves and

$$\rho_{TM} = \frac{\epsilon^{-1/2} \cos \theta + j(\epsilon \sin^2 \theta - 1)^{1/2}}{\epsilon^{-1/2} \cos \theta - j(\epsilon \sin^2 \theta - 1)^{1/2}} \tag{73}$$

for the H_y component of TM waves. The imaginary terms in (72) and (73) represent an exponential decay of the fields outside the dielectric. The propagation coefficient in the x direction is real and given by

$$\gamma = -(2\pi/\lambda)(\epsilon \sin^2 \theta - 1)^{1/2}. \tag{74}$$

The reflection coefficients always have a magnitude of unity and thus transverse standing waves are set up in the dielectric which are cosinusoidal for odd-numbered modes and sinusoidal for even-numbered modes. The electrical length ϕ of the standing wave from the midplane to the boundary for both TE_{0n} and TM_{0n} modes is given by

$$\phi = \cos^{-1}\left|(1 + \rho)/2\right| + (n - 1)\pi/2. \tag{75}$$

If λ_x is the transverse wavelength, Fig. 18(a) gives

$$\lambda/\lambda_x = \epsilon^{1/2} \cos \theta \tag{76}$$

and, therefore,

$$\lambda_x/l = 2\pi/\phi. \tag{77}$$

Combination of (76) and (77) gives

$$\lambda/2l = (\pi\epsilon^{1/2} \cos \theta)/\phi. \tag{78}$$

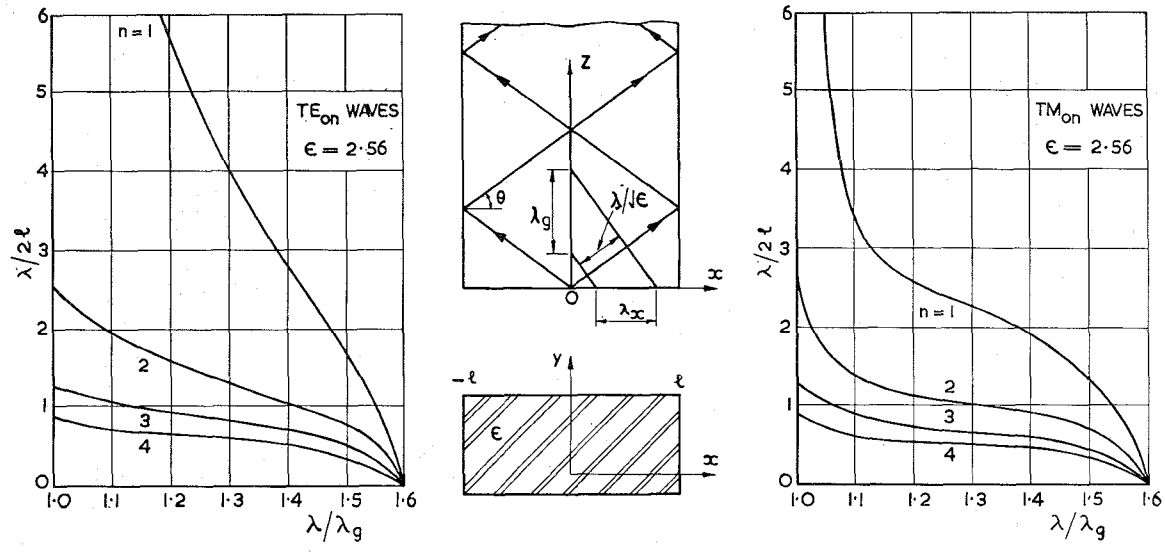

(a) (b) (c)

Fig. 18—Propagating modes in dielectric sheets. (a) Guide wavelength for TE_{0n} modes. (b) Geometry of the system. (c) Guide wavelength for TM_{0n} modes.

At cutoff, $\phi = 0$ and $\cos\theta = [(\epsilon-1)/\epsilon]^{1/2}$ so that

$$\frac{\lambda_c}{2l} = 2\frac{(\epsilon-1)^{1/2}}{n-1}. \tag{79}$$

Thus, for a given value of λ/λ_g, θ may be found from (69) and ϕ from (75) to give $\lambda/2l$ from (78). Values of $\lambda/2l$ vs λ/λ_g are plotted for polystyrene material with $\epsilon = 2.56$ in Figs. 18(b) and 18(c) for various TE and TM waves.

Cylindrical Rods

The theory of the nonradiative modes propagated along a dielectric rod was give by Hondros and Debye [115] and confirmed experimentally by Zahn [290] and Schriever [225]. Their study has a long history [53], [153], [209], [217], [218], [234] and is still the subject of extensive investigation [1], [127], [128], [249], [286]. A typical analysis [40], [78] assumes that there is a cylindrical coordinate system r, θ, z having its z-axis along the rod of radius r_1. The longitudinal components of the field vectors, omitting the factor $e^{(j\omega t-\gamma z)}$ are, inside the rod with $r < r_1$,

$$E_{zd} = A\cos n\theta J_n(u_d r), \tag{80}$$

$$H_{zd} = B\sin n\theta J_n(u_d r), \tag{81}$$

where

$$\gamma^2 - u_d^2 = -\epsilon\omega^2/c^2. \tag{82}$$

Outside the rod, with $r > r_1$,

$$E_{za} = C\cos n\theta H_n^{(1)}(ju_a r), \tag{83}$$

$$H_{za} = D\sin n\theta H_n^{(1)}(ju_a r), \tag{84}$$

with (30) as previously. Similar relations hold for the other field components. Eqs. (30) and (82) give

$$[(u_d^2 + u_a^2)/(\epsilon - 1)]^{1/2} = \omega/c. \tag{85}$$

A further relation between u_d and u_a is obtained from the boundary conditions and thus enables these quantities to be obtained for given values of ω, n, and ϵ.

For $n = 0$, the fields as shown in Fig. 19(a) are rotationally symmetrical and there are two solutions. One corresponds to a TM mode in which the magnetic lines of force are circles centered on the rod axis. The electric lines of force lie in the meridional planes through the rod axis; they go to infinity and asymptotically approach planes perpendiuclar to the rod that are spaced $\frac{1}{2}\lambda_g$ apart. The other solution corresponds to a TE mode in which the roles of the magnetic and electric field vectors are interchanged. If $n = 1$, there is an unsymmetrical or "dipole" wave which may be roughly described as a sinuosidal dielectric polarization perpendicular to the rod and travelling along it. There is no cutoff frequency for this wave, which thus exists for thin rods or low frequencies.

The guide wavelength is given as a function of rod radius in Fig. 19(b) for the $n = 0$ and $n = 1$ modes, the free-space wavelength being 1.25 cm and $\epsilon = 2.56$ for polystyrene. The attenuation coefficient is given in decibels per meter by

$$\alpha_d = 2729\epsilon(F/\lambda)\tan\delta, \tag{86}$$

where F is a dimensionless quantity plotted in Fig. 19(c). For large radii of the rod, F tends to its plane-wave value of $\epsilon^{-\frac{1}{2}} = 0.625$ while for thin rods, it becomes smaller because a greater fraction of the energy resides in the external medium. Nonradiative modes similar to those discussed can also exist on dielectric tubes [264].

The $n = 0$, TM mode on a dielectric rod can be launched [123] from the end of a TEM mode coaxial line or a TM mode circular waveguide [7]. The $n = 0$, TE mode can be excited from a similar plate containing

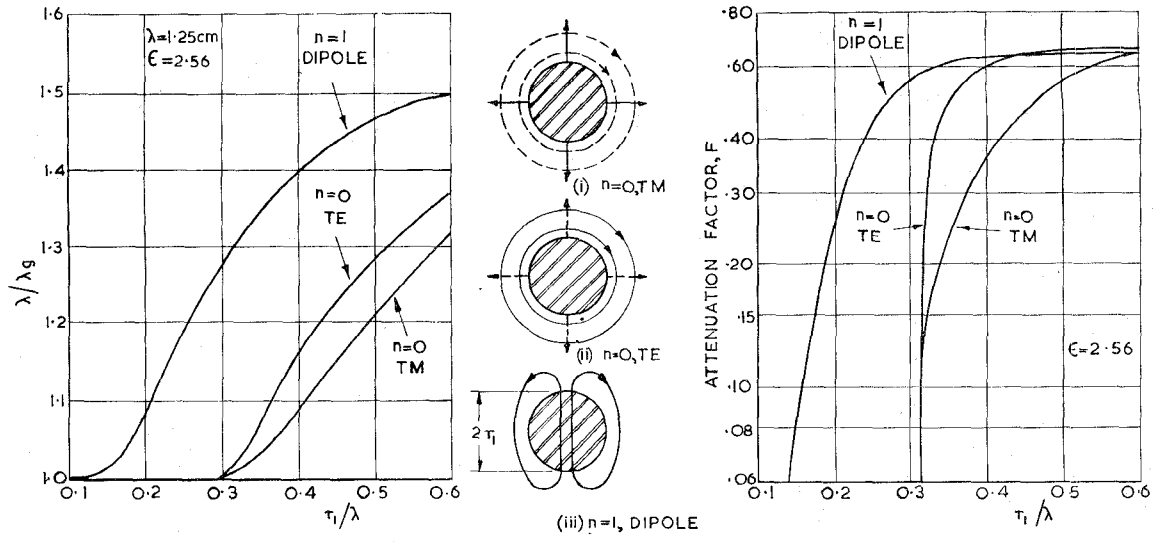

Fig. 19—Propagation along dielectric cylinders. (a) Field configurations of various modes. (b) Guide wavelength vs radius. (c) Attenuation vs radius.

slots which are suitably orientated and excited. The field configurations of the $n=1$, dipole, or HE_{11} mode are roughly similar to those of the TE_{11} mode in circular waveguide, and, thus, a suitable transition is one in which the dielectric rod, tapering from a point to minimize reflection, is inserted in the guide to fill the open end. The portion of the rod external to the guide may be further tapered to any size required. An experimental investigation [41] of this mode at 24 kmc showed that the guiding effect was retained even when the rod was only a fraction of a wavelength in diameter. With polystyrene material, the attenuation coefficient could be as small as 0.004 db/m, the values showing good agreement with (86). A length of the dielectric rod made resonant by supporting it between two plane mirrors 36-inches square, gave a maximum Q factor of 53,000. The propagation in the dielectric is, of course, altered by shielding [259] the rod by a metal tube.

In the case of TM modes supported by a lossy dielectric, it may be shown [18] that when the radius of the rod exceeds a certain value, the surface impedance is inductive and when it is less, the surface impedance is capacitive. For a perspex rod, $\epsilon=2.61$, radius 0.978 cm, the phase velocity at frequencies below 9.2 kmc was greater than the velocity of light.

Multiple Media

Surface waves may be propagated under more complicated conditions than those considered so far. In particular, the properties have been analysed of a cylindrical conductor embedded in two [122] or three [43] layers of coaxial dielectric. An analysis of surface wave propagation along several layers of different media has been given by Karbowiak [137] who showed that the surface impedance is then given by the sum of the surface impedances of the individual layers taken by themselves each over a perfectly conducting sheet. Furthermore, the impedance will remain the same even if one layer of the composite medium is split up into a number of thinner layers and intermixed with the others; it is the total thickness of any one medium that is important.

The analysis becomes difficult when the conductor is coated with a slab of magnetized ferrite. For thin slabs, the TM mode is dominant and if the applied steady field is perpendicular to the surface, it may be shown [195] that the phase velocity can be controlled by variation of its magnitude.

Provided that the dielectric coating on the conductor is thick enough, the higher order modes found in the case of the plain slab can propagate. The electric and magnetic fields have one or more half-sinusoidal variations in the dielectric but decay exponentially in the external air medium. The TM modes were given in an unpublished work by R. B. R. Shersby-Harvie by p_n, the $(n+1)$th solution of

$$\tan\left[2\pi p_n(\epsilon_d - 1)^{1/2}\frac{l}{\lambda}\right] = \epsilon_d\left(\frac{1}{p_n^2} - 1\right)^{1/2}. \quad (87)$$

The cutoff wavelength for the nth mode is given by

$$\lambda_c = 2l(\epsilon_d - 1)^{1/2}/n \quad (88)$$

and the corresponding guide wavelength is given by

$$\left(\frac{\lambda}{\lambda_g}\right)^2 = 1 + (\epsilon_d - 1)(1 - p_n^2). \quad (89)$$

Propagation is possible at all frequencies when $n=0$; this is the TM_0 mode previously considered for thin layers.

For TE modes, p_n is a solution of

$$\cot\left[2\pi p_n(\epsilon_d - 1)^{1/2}\frac{l}{\lambda}\right] = -\left(\frac{1}{p_n^2} - 1\right)^{1/2}. \quad (90)$$

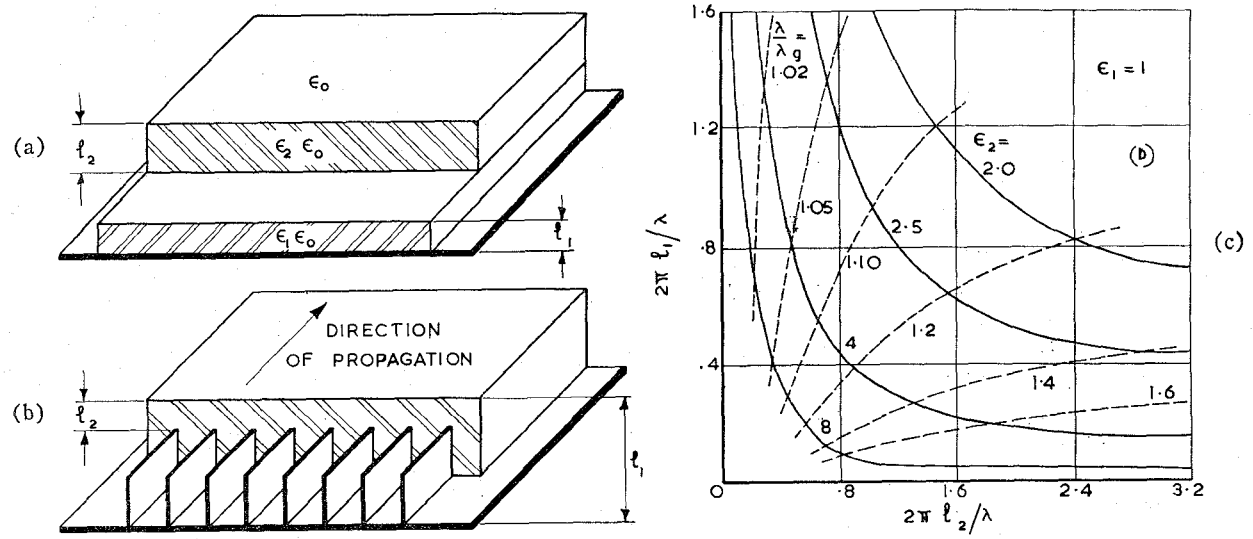

Fig. 20—Arbitrary-polarization surface-wave structures. (a) Double-dielectric slab. (b) Contours of equal phase velocity for TM and TE modes. (c) Single-dielectric slab with septa.

This has no real solutions if l is sufficiently small so that the lowest mode in this case has a cutoff wavelength. For the nth mode

$$\lambda_c = 4l(\epsilon_d - 1)^{1/2}/(1 + 2n) \tag{91}$$

and the corresponding guide wavelength is given by

$$\left(\frac{\lambda}{\lambda_g}\right)^2 = 1 + \left(\frac{\lambda_c}{4l}\right)^2 (1 + 2n)^2(1 - p_n)^2. \tag{92}$$

For some applications of surface-wave structures it is desirable to support a wave of arbitrary polarization; this means the combination of two principal polarization components with arbitrary amplitudes and phase. Propagation of such a wave over a surface-wave system requires that both TM and TE waves be supported and also possess the same propagation coefficient. The general equations for an n-layered slab have been given [75] and it has been shown [205] that the requirements for arbitrary polarization can be met by the double-layer earthed dielectric slab shown in Fig. 20(a). Typical contours of equal phase velocity for TM and TE waves on the slab-thickness plane are given [205] in Fig. 20(b); the lower slab is air filled, the parameters are λ/λ_g, and ϵ_2 is the dielectric constant of the upper slab.

A corrugated surface is unable to support a TE mode and thus an alternative medium for arbitrary polarization involves [108] the use of a "mode filter" consisting of septa embedded within a single dielectric slab whose initial thickness l and dielectric constant are adjusted for a given "trapping" of the TE mode. The septa shown in Fig. 20(c) are spaced considerably less than $\frac{1}{2}\lambda$ in the dielectric medium so that a wave with the electric field polarized parallel to them is reflected. The height $(l_1 - l_2)$ of the septa is chosen so that the TM mode is "trapped" to the degree desired. For example, with a slab of dielectric constant 2.5, an inverse velocity ratio (λ/λ_g) of 1.2 is obtained with a slab thickness $2\pi(l_1 - l_2)/\lambda = 1.0$ for the TM mode and $2\pi l_1/\lambda = 2.1$ for the TE mode. Such equal velocity surfaces are, of course, able to support circularly-polarized waves.

Image Lines

Surface-wave systems have found their main application in the antenna field [107] but the dielectric image line of King [146] shown in Fig. 21(a) has several advantages as a transmission line. This image line is essentially a dielectric rod supporting, as in field configuration (iii) of Fig. 19(a), the dipole mode in which a conducting sheet is placed in the plane of symmetry and normal to the electric field. Thus half the rod and the space surrounding it are replaced by an image in the conductor.

The polarization of such a line is uniquely determined while the phase-change coefficients are identical to those of the complete rod. The extent of the RF fields is determined by the ratio of rod radius to wavelength; if for example, this is 0.142, then 80 per cent of the power flows in a region of radius ten times that of the rod. For $\lambda = 1.25$ cm, a typical line in polystyrene would have a radius of 2 mm, the total width of the image plane being 10 cm.

The loss in the dielectric material is given by (86) but is supplemented by losses caused by radiation and the finite conductivity of the image plane. In the absence of artificial boundaries to the field, the radial component of the Poynting vector is purely imaginary and the radiation is zero. Loss caused by radiation does, however, occur in the presence of bends, obstacles and a finite image surface. The attenuation coefficient caused by conductor loss is given in decibels per meter by

$$\alpha_c = 69.5R_sF'/\lambda Z_a, \tag{93}$$

where F' is a factor which must be calculated [149] for

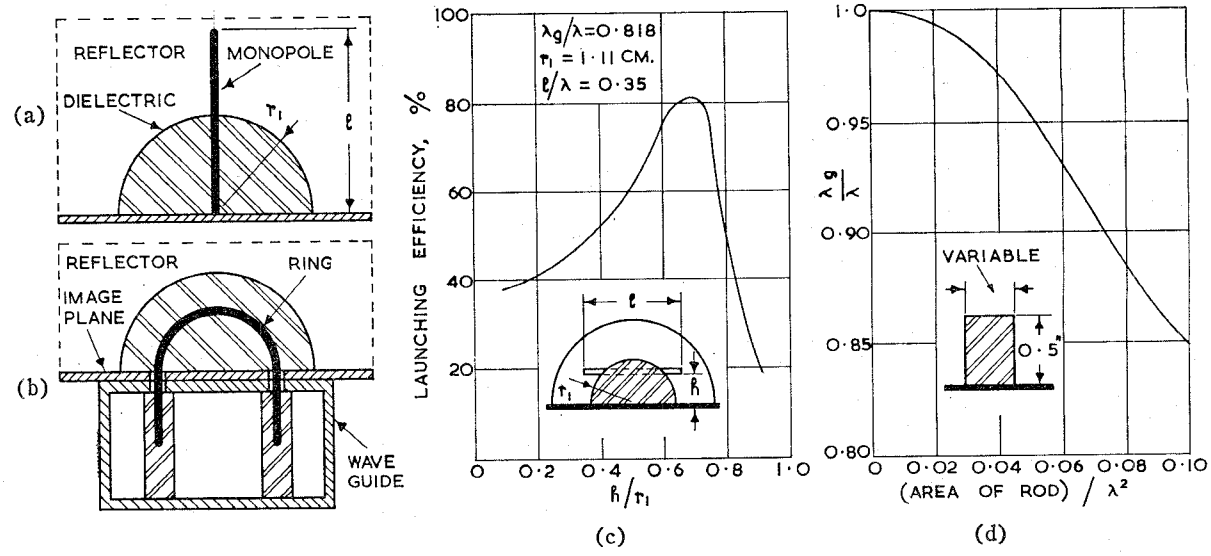

Fig. 21—Dielectric image lines. (a) Monopole launching. (b) Ring launching. (c) Efficiency of slot excitation. (d) Effect of varying the area of a rectangular rod. The frequency is 9.7 kmc.

the particular geometry. This loss is generally smaller than that caused by the dielectric except when the wave is only loosely bound to the line. For example, at 9.6 kmc the total attenuation coefficient in decibels per meter is 4.0 and 0.2 for values of r_1/λ of 0.4 and 0.15, respectively.

There are several methods of efficiently launching [73] a pure dipole mode on an image line. The monopole in Fig. 21(a) achieves an efficiency of 75 per cent provided that l/λ exceeds 0.15. It is necessary to position a reflecting plate about $\frac{1}{4}\lambda$ behind the monopole. As shown in Fig. 21(b), a ring excited from a rectangular waveguide achieves 75 per cent efficiency for r_2/λ between 0.1 and 0.2. The efficiency of resonant-slot excitation as a function of distance from the image plane is shown in Fig. 21(c).

The small dielectric cross sections used in the dipole mode do not permit any transverse resonances within the dielectric and the concentration of the field about the rod depends upon the volume of dielectric in regions of high electric field. The properties of the transmission system should therefore be insensitive to the exact shape of the dielectric cross section, but strongly dependent upon the total cross-sectional area occupied by the dielectric. Typical sections studied [147] at a frequency of 24 kmc were a half round, radius 0.066 inch, both in the normal and inverted positions, a 0.084-inch square, and a rectangle, 0.280 inch×0.030 inch, with either face in contact with the image plane. Such shapes, as well as recessed and twin lines, all show much the same dielectric loss and field confining effect. The rectangular shape does, however, lend itself to easy fabrication and Fig. 21(d) gives data [223] at 9.7 kmc for a particular sample.

Experiments [148] show that the system is insensitive to minor twists and imperfections in the dielectric rod while the surface finish of the image plane is not important. Such properties make the image line suitable [289] for millimeter wavelengths. Simple bends and corners can be made with moderate loss and low reflection. Semiconductor diodes may be coupled to the image line with an insulated metal pin to give a VSWR better than 1.2. A variable attenuator results when a thin resistive sheet is placed in a radial plane whose angle with respect to the image plane can be adjusted. Such devices as standing-wave meters and directional couplers can also be made in image line.

Coupled-Resonator Structures

Tape-Ladder Lines

Systems propagating slow electromagnetic waves are used extensively in practice and, although continuous dielectrics have a limited application, the majority employ periodic structures of various kinds [26], [106], [130]. The velocity of propagation in such structures must depend upon the particular application and may, for example, be c for linear electron accelerators [110], 0.1 c for electron-tube amplifiers [202] and 0.01 c for solid-state low-noise amplifiers [68]. Although bidimensional and tridimensional slow-wave structures have been examined [30], [182], only linear types will be considered in what follows.

The power P flowing along a slow-wave structure and W_s are related by

$$P/W_s = v_g. \tag{94}$$

If the electric field in the structure is of importance, then a practical parameter is the coupling impedance

$$Z_c = |E|^2/2\beta^2 P. \tag{95}$$

If the modulus of the magnetic field is effective, the performance is specified by the admittance

$$Y = |H|^2/2\beta^2 P. \tag{96}$$

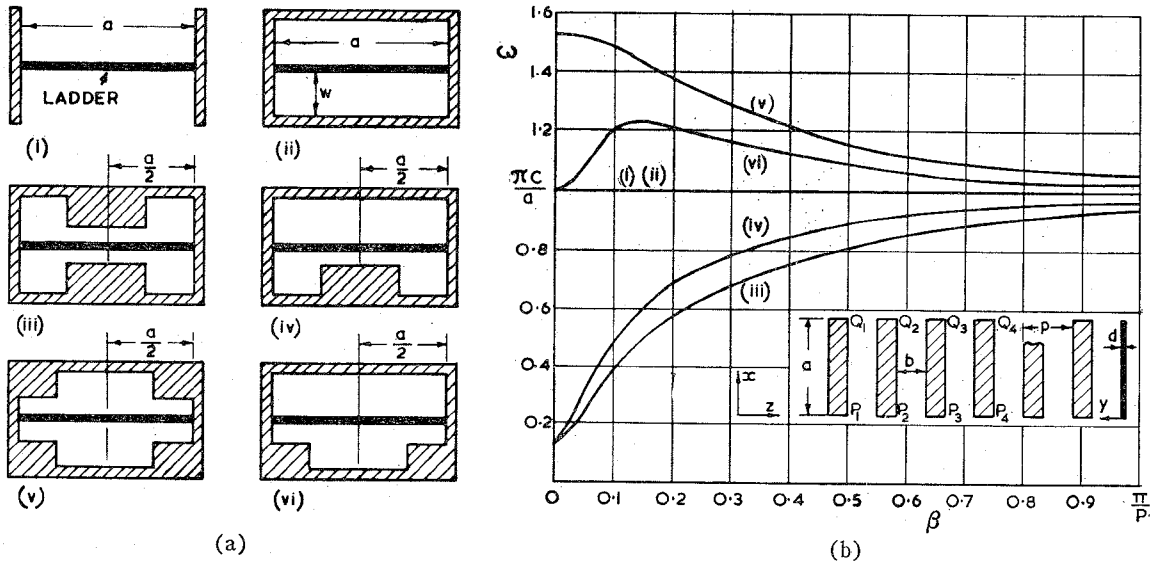

(a) (b)

Fig. 22—Propagation along tape ladder lines. (a) Cross sections of lines. (b) Dispersion curves with ladder detail. Structures are (i) side wall, (ii) waveguide, (iii) double ridge, (iv) single ridge, (v) double tee and (vi) single tee.

Another parameter, the shunt impedance, is defined as

$$Z_{sh} = |E|^2/2\alpha P \tag{97}$$

and is related to the power dissipated per unit length because of ohmic losses.

A large class of slow-wave structures consists [21] of resonators of identical shape and size coupled together. The two basic types of coupling are pure inductive and pure capacitive, the magnitude of each component determining how the ω-β diagram of the uncoupled resonators is modified. For example, the ladder line consists, as shown in the inset of Fig. 22(b), of a periodic array of parallel straight conductors. Such a wire or tape structure can propagate a variety of TEM waves, each one corresponding to a different mode of excitation of the tapes; the simplest mode is that in which there is a phase change βp from one tape to the next.

$$V_m \text{ (or } I_m) = V_{m-1} \text{ (or } I_{m-1}) e^{-i\beta p}. \tag{100}$$

The characteristic impedance of a single conductor in the array may be defined by

$$Z_0(\beta p + 2n\pi) = V_m/I_m, \tag{101}$$

where n is caused by the periodicity of the structure.

The method of determining Z_0 found by Fletcher [85] is restricted to rectangular conductors and assumes that the component E_z of field is constant throughout the region between the tapes. The fields at the common boundaries of the other regions are then matched. The voltage on the nth conductor can then be obtained directly, and the current in the conductor can be found by integrating the tangential component of magnetic field around its periphery. With the ladder equally spaced from either ground plane and with dimensions as in Fig. 22, this method gives

$$\frac{Z_w}{Z_0} = \frac{4d}{b}\sin^2\left(\tfrac{1}{2}\beta p\right) + 4\left(1-\frac{b}{p}\right)\sin\left(\tfrac{1}{2}\beta p\right)\sum_{-\infty}^{+\infty}(-1)^n \times \coth\left\{\frac{w}{p}(bp+2n\pi)\right\}\frac{\sin\left\{\left(1-\frac{b}{p}\right)\left(\frac{\beta b}{2}+n\pi\right)\right\}}{\left(1-\frac{b}{p}\right)\left(\frac{\beta p}{2}+n\pi\right)}\cdot\frac{\sin\left\{\frac{b}{p}\left(\frac{\beta p}{2}+n\pi\right)\right\}}{\frac{b}{p}\left(\frac{\beta p}{2}+n\pi\right)}. \tag{102}$$

The dispersion curve and coupling impedance of the ladder structure can be calculated by assuming that the TEM-mode voltage on each wire is given by

$$V(x, y, z, t) = V(y, z)(Ae^{-i\beta_w x} + Be^{i\beta_w x})e^{i\omega t}, \tag{98}$$

where

$$\frac{\partial^2 V}{\partial y^2} + \frac{\partial^2 V}{\partial z^2} = 0. \tag{99}$$

The voltage and current on successive conductors in a given (y, z) plane are related by

Numerical values of the summation for practical geometries have been given by Walling [276]. If $w/p \to 0$, (102) simplifies to

$$\frac{Z_w}{Z_0} = \frac{4d}{b}\sin^2\left(\tfrac{1}{2}\beta p\right) + \frac{2p}{w}\left(1-\frac{b}{p}\right). \tag{103}$$

Leblond and Mourier [163] calculated Z_0 by using a quasi-electrostatic field distribution in the (y, z) plane, but this method requires a measured value of the capacitances between different parts of the structure. The

analysis also assumes that the conductors are thick enough in the direction normal to the plane of the ladder to ensure that each wire is shielded from all except its neighbours; for rectangular conductors the result reduces to (103).

Butcher [38] has exactly calculated the RF fields distributed around an array of thin tapes by a method which takes into account all the mutual couplings. This theory predicts in the practical case of equal tape and gap widths with $w = \infty$ that

$$\frac{Z_w}{Z_0} = 4 \sin \tfrac{1}{2}\beta p \tag{104}$$

which may be compared with (102). It was shown that the coupling impedance and the group velocity have a product which with certain provisos, is the same for a wide range of geometries. This "field distribution factor" of an array, using (94) and (95) is given by

$$F_d = \frac{v_g Z_c}{c Z_w} = \frac{\epsilon_0 |E|^2}{2\beta^2 W_s}. \tag{105}$$

In the case of space harmonics such that $1.5\pi < \beta < 2\pi$, the exact solution leads to much higher values for the coupling impedance than those given by the approximate methods.

The results of these methods are applied to practical structures by consideration of the geometry and boundary conditions. In Fig. 22(a) the tapes are short-circuited at either end by (i) two perpendicular conducting side walls or (ii) the opposing narrow walls of a rectangular waveguide. Whatever the value of β, this array can support TEM standing waves only at the frequency for which λ is twice the length of the tapes. The dispersion curves (i) and (ii) shown in Fig. 22(b) are thus horizontal lines and since the group velocity is always zero, the structure does not propagate. Both inductive and capacitive coupling are present but the amounts are just equal and cancel each other.

The tape-ladder line can be given a pass band with finite bandwidth by upsetting [37] the equality. The frequency corresponding to any value of β can be reduced by distorting the structure to the ridge shapes (iii) and (iv) of Fig. 22(a) which, in effect, reduces the cutoff frequency of the guides formed on either side of the ladder. The dispersion curves therefore have the forms labelled (iii) and (iv) in Fig. 22(b) and the structure now propagates energy. The frequency corresponding to any value of β can be increased by adopting the tee-shaped structures (v) and (vi) of Fig. 22(a), the corresponding dispersion curves being given in Fig. 22(b). The single tee curve behaves peculiarly because the cutoff frequency of the TE_{01} mode of the guide formed below the ladder is higher than the zero mode cutoff frequency set by the guide above the ladder and the first resonant frequency of the tapes. In both tee structures the fundamental is seen to have the phase and group velocities in opposite directions; it is thus a backward wave. The π-mode cutoff frequency of any of these ladder lines can be raised by using shorter tapes running between horizontal plates supported by the side walls [186]. The π-mode cutoff frequency is still approximately equal to the first resonant frequency of the short-circuited tapes and is thus inversely proportional to their length. This is a valuable technique for broadening the pass band of these structures while, moreover, energy can now be made to propagate down the undistorted rectangular waveguide.

The above analysis can be applied to a structure consisting of two parallel arrays. In this case, modes can exist with symmetric or antisymmetric field distributions; the former is usually of practical interest. Such multiple lines give [191] high coupling impedance, wide pass band, and low dispersion. Ash [11] has shown that propagation takes place along the ladder if the tapes are inclined or distorted in some way. Since there is now no need for ridge or tee sections, several ladder lines may be stacked together. Tape-ladder lines have proved to be a convenient means of achieving [68] group velocities of the order of 0.01 c.

If, in the ladder line of the inset of Fig. 22(b), P_1 is short-circuited to P_3 and Q_2 is short-circuited to Q_4, while P_2, P_4, Q_1, and Q_3 are open-circuited and so on down the array, the interdigital line [112], [164], [193], [279] of Fig. 23(a) is obtained. The period of the whole structure is $2p$, but it is also unchanged when it is moved along the z-axis through half a period and then reflected in the $x = 0$ plane. It is possible, therefore, to consider a mode for which the electric field at $(-x, y, z+p)$ differs from that at (x, y, z) only by a constant factor $e^{-j\beta p}$.

Taking into account the boundary conditions, the dispersion curve may be calculated as for the ladder line. The results [38] for thin tapes, for various values of b/p, are given in Fig. 23(b). The branch corresponds to a backward space harmonic but the complete dispersion curve can be obtained by displacing it by integral multiples of π/p along the β-axis and then reflecting all these branches in the ω-axis. The portions of the curve in which v_g tends to be greater than c lie in forbidden regions such that the phase velocity of one of the space harmonics also exceeds c. The exact dispersion curve of a completely open structure cannot pass through the forbidden regions because, if it did, the structure would radiate. For thick tapes, successive gaps are shielded from one another and the structure resembles a folded transmission line; the branches are given by

$$\pm \omega - 2\beta = 2n\pi/p \tag{106}$$

as shown by the dashed line of Fig. 23(b). For very wide gaps, the free-space wavelength has the value $4a$ as in the dotted line.

The meander line of Fig. 23(c) is constructed by short circuiting P_1 and P_2, Q_2 and Q_3, and P_3 and P_4, and so on down the array. The structure has a period of $2p$ and is able to propagate at frequencies down to zero. It may

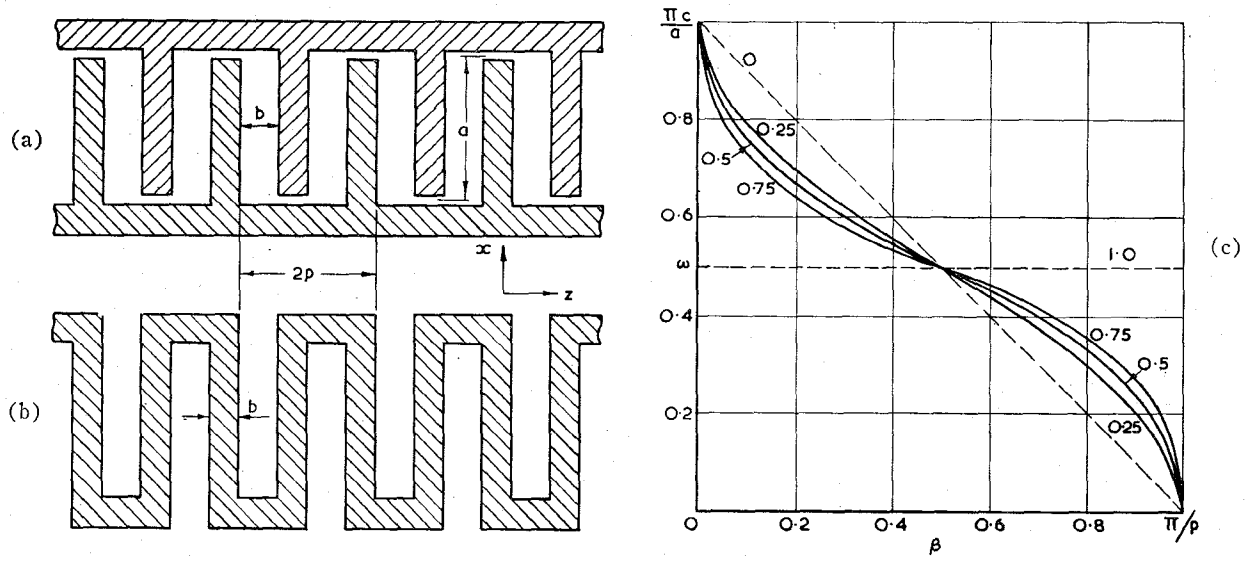

Fig. 23—Interdigital and meander structures. (a) Interdigital tape line. (b) Dispersion curves with parameter b/p. (c) Meander tape line.

be shown [38] by the use of Babinet's principle that the complete dispersion curve of a meander line with gap width $(p-b)$ and tape width b is the same as that of an interdigital line with gap width b and tape width $(p-b)$. For structures with thick tapes, the phase velocity of the nth space harmonic is given by

$$\frac{c}{v_{pn}} = 1 + \frac{a}{p} + \frac{\lambda}{2p}(2n-1) \tag{107}$$

and the group velocity is

$$v_g = \frac{c}{1 + a/p}. \tag{108}$$

Resonant Cavities

Slow-wave structures [65], [66] may employ resonant cavities coupled in various ways. If the amount of loading is small, the analysis can be based on a perturbation of a homogeneous transmission line. For example, Field [82] considered a coaxial line in which either the inner or outer conductor is provided with radial grooves [70], [242]. Such an inductively-loaded surface can support a TM-type slow wave, the phase velocity being governed by the depth of the stub. At 9 kmc the inner conductor is typically 0.686-inch diameter with disk thickness of 0.011 inch and spacing rather more. As with all corrugated structures, the field decays in the transverse direction and, in the example quoted, the field is effective to about 0.04 inch from the disc edges.

The structure of Fig. 24(a) is essentially a rectangular waveguide with one broad wall inductively loaded with series stubs. The dispersion curve resembles that of Fig. 2 except that there is a lower cutoff frequency caused by the unperturbed waveguide. A waveguide of square section can transmit two orthogonal modes with different velocities and, as such, is a broad-band means of producing [236] circularly polarized waves. In practical

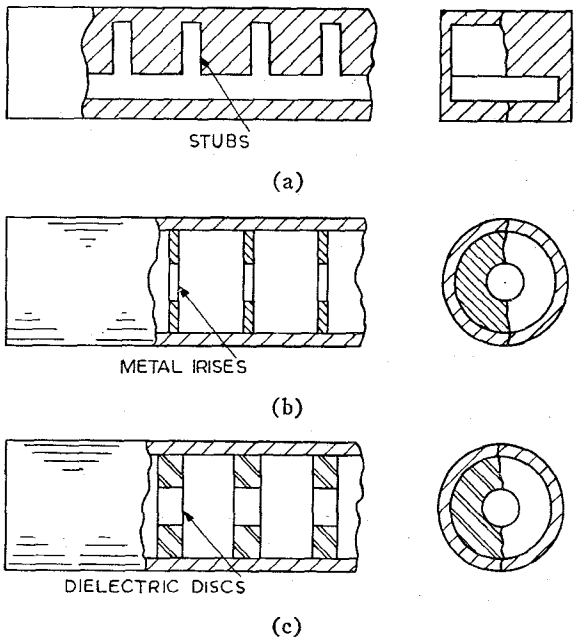

Fig. 24—Coupled-cavity slow-wave structures. (a) Stub resonators in rectangular guide. (b) Capacitive-coupled circular resonators. (c) Dielectric-disc loading of circular guide.

structures [135], [179], [265] for millimeter wavelengths the stubs have been milled in the ridge of a ridged waveguide.

The disk-loaded circular guide [144], [201] of Fig. 24(b) has been extensively employed in applications requiring $v_p = c$. The theory [31], [51], [69], [101], [102], [104], [105] of TM propagation is based on a matching of the fields at the mouths of the resonators. The dispersion [56], [245], [268], [269], [270] of this structure is rather pronounced but can be reduced at the expense of low coupling impedance by the use of large apertures in the disks. Data has been given on attenuation [57] and the theory has been confirmed by

experiment [103]. An alternative treatment assumes [165], [181], [233] that the circular waveguide is periodically loaded with shunt susceptances while an accurate estimation of the dispersion curve has been based [212] on a Fourier series representation. In some cases, lower attenuation is achieved by the use of dielectric disks [277], [278] as an anisotropic artificial medium.

Resonant-cavity slow-wave structures can be analysed [21] by consideration of the method of coupling. Pure inductive coupling is a scheme in which only H lines link the cavities. An example consists of a TE_{01} mode rectangular waveguide with transverse partitions spaced distance p apart. The dispersion curve is a horizontal frequency line corresponding to $\lambda_g = 2p$ which joins the points at $\beta = 0$ when the cavities oscillate in phase and at $\beta = \pi$ when they are out of phase. Narrow slots in the partitions cut centrally and parallel to the short sides of the guide allow inductive coupling, and consideration of the magnetic field distribution shows that the π mode is not affected whereas the zero mode is lowered until, as the slot widens, it reaches the cutoff frequency of the plain rectangular waveguide. The equivalent circuit of this structure is a transmission line periodically loaded with shunt inductances and the dispersion curve thus resembles that of Fig. 2.

Pure capacitive coupling exists in the disk-loaded circular waveguide, since E lines penetrate the small central aperture. In this case the zero mode is not disturbed while the other end of the pass band rises as the hole diameter increases to reach eventually the characteristic of a plain circular guide. The equivalent circuit of this structure is that of a line loaded with shunt capacitance and the dispersion curve resembles that of Fig. 1.

Mixed coupling is characterized by the presence of both E and H lines in the coupling mechanism. Again considering the disk-loaded circular waveguide, a slot cut in the periphery of the partitions will introduce inductive coupling. Investigation of the field perturbations caused by the central and peripheral apertures shows that the zero mode remains constant while the π mode is raised in frequency for the capacitive coupling, as previously observed, but lowered for the inductive coupling. If the structure initially has a central aperture, the addition of the inductive slot will decrease the capacitive pass band until, with equality of coupling, it becomes zero. Further increase in size of the inductive slot, which may be regarded as introducing positive mutual coupling, lowers the π-mode frequency. The fundamental component of the wave travelling through the structure now has negative phase velocity [48] and is thus a backward wave.

In disk-loaded circular guides employing an electron beam, less stringent requirements are placed on the central aperture if the coupling of the cavities is mainly by inductive slots. Forward-wave operation now requires, however, the use of the $n = +1$ space harmonic with consequent reduced coupling impedance. A forward-travelling fundamental may be set up by employing negative mutual coupling. Chodorow and Craig [47] achieved this by using different shapes for alternate cavities so that the magnetic field on opposite sides of the partition is in the same direction at the π mode but in the opposite direction for the zero mode. The cloverleaf structure [47], [91] of Fig. 25(a) is an example of such a design. The dispersion curve shows that the zero-mode frequency is depressed relative to the π mode. At $\beta p = \frac{1}{2}\pi$, a typical coupling impedance is about 130 ohms.

Negative mutual coupling can also be obtained [47] with the structure of Fig. 25(b) in which adjacent cavities are coupled by reversed loops. An extension of this principle is that with the addition of many loops around the entire structure, the metallic wall can then be omitted. The dispersion curve of such an interlaced structure, shown in Fig. 25(b), indicates that the fundamental is again a forward wave. For reference, the cutoff frequency of the TM_{01} mode in the unloaded guide is also given. The characteristics are modified [194] when the loop circuits are themselves resonant.

The characteristics of periodically loaded waveguides may be measured by a number of experimental methods [9], [79], 159], [247]. The properties of a matched input coupling [185] may be examined by terminating the slow-wave structure with a nonreflecting load and by making impedance measurements in the input transmission line. In one method [124], all reactive values of the impedance in the loaded guide were produced by sliding a metal shorting plug into it at various distances. The parameters of the coupling system were then determined by the well-known nodal shift method.

The frequency characteristic of a periodic guide may be determined from probe measurements when the far end is short circuited. Care must be taken in the location of the probe since it detects the total electric field of all the space harmonics whereas generally a determination of the wavelength of the fundamental space harmonic is all that is required. Another method makes use of the fact that the phase of the field inside the stub uniquely determines the fundamental wavelength in the line. Thus by measurement of the amplitudes of the fields at the back of each stub and plotting on a graph, the wavelength may be obtained. Greater accuracy was obtained [135] in measurements at 50 kmc by using a sliding base plate to carry the probe, the output of which was fed into a bridge comparison circuit.

One satisfactory method is to short circuit the transmission system at both ends and to search for the resonant frequencies of this structure. It is necessary that the short-circuiting plungers be at planes of symmetry of the system so that all space harmonics have zeros in the standing-wave pattern at the plungers. If this is not done, reactances, caused by other modes being excited at the ends of the structure, would result in the resonant frequencies being dependent to some extent on the

length of guide chosen. The condition for resonance is that there must be an integral number of half-wavelengths in the length of the guide so that for a structure of N resonators, β is given by

$$\beta = 2\pi/\lambda_g = n\pi/Np. \tag{109}$$

The resonant frequencies of the author's structure consisting of $N=6$ resonators are shown in Fig. 26; the relevant dimensions are given in the inset. It is seen that the modes form a group of $N+1$ frequencies in a restricted pass band where the modes are clustered in the neighbourhood of the two edges of the pass band and more widely spaced between. The edges of the pass band are the zero and π modes at which the phase changes from one section to the next are $\beta p=0$ and π, respectively. The group velocity may be found from the slope of the curve and therefore by using a measured value of unloaded Q factor, the attenuation is calculated from (8). A periodic waveguide may also be made resonant by bending it around in a circle so that the input connects to the output. In this case there must be an integral number of whole wavelengths in the length of guide and, once again, the continuous curves break up into a series of discrete points or modes. In both these types of resonators the separation of the resonances, especially near the π mode, can be increased by the use of systematically-modified loading reactances.

The field distribution, coupling impedance, and shunt impedance of a slow-wave structure are usually determined by perturbation techniques [3], [184]. As shown

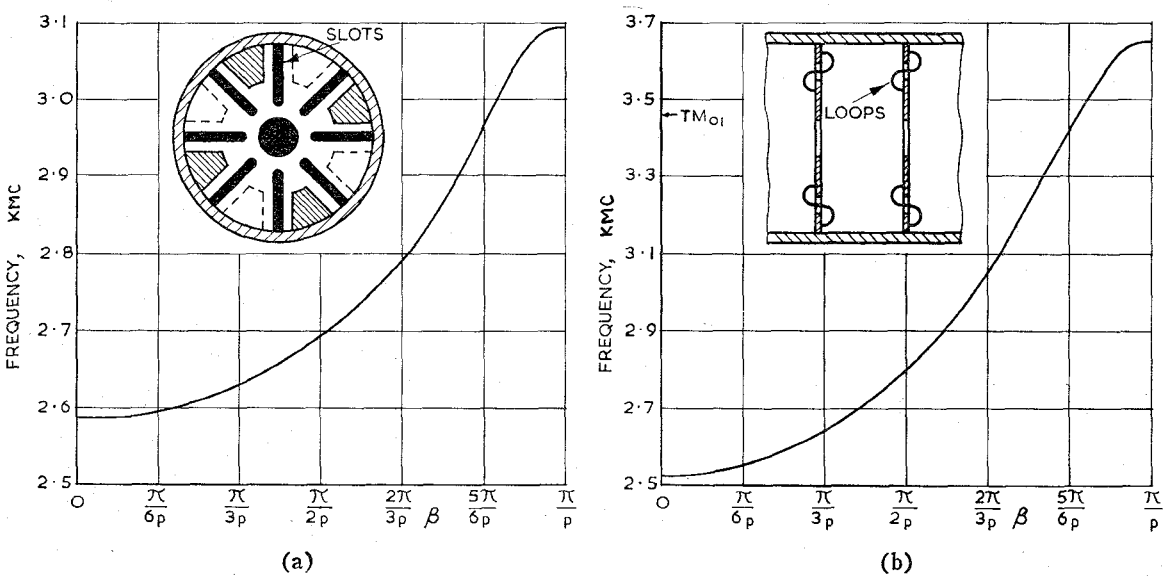

Fig. 25—Slow-wave structures with negative-mutual inductance coupling. (a) Re-entrant cavity with slot coupling. (b) Cavity with reversed-loop coupling.

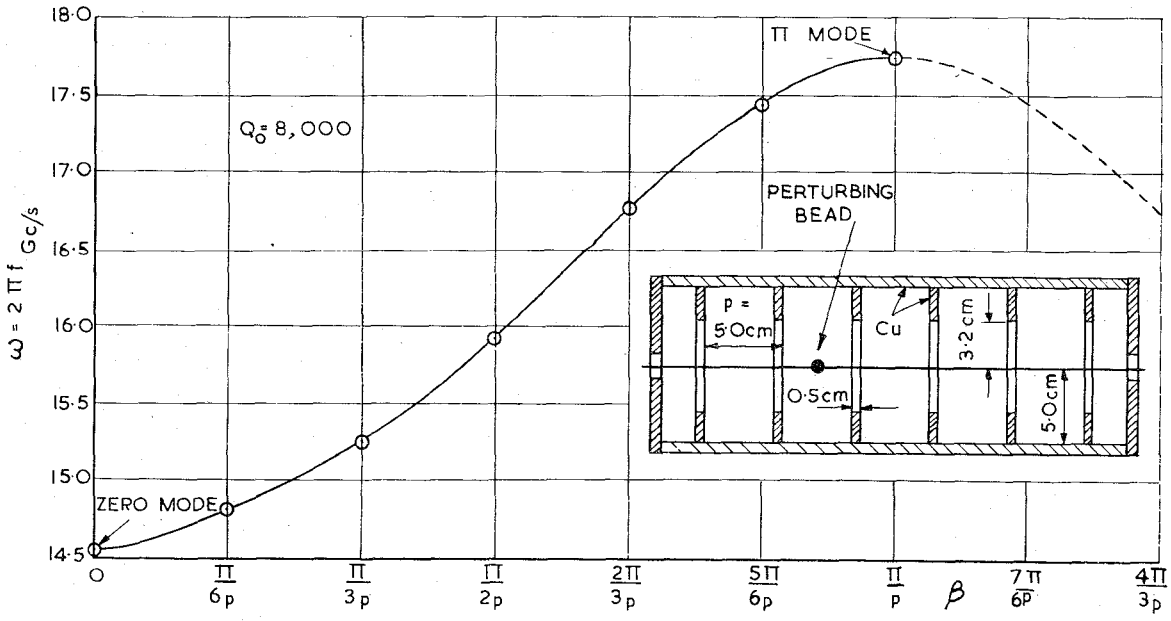

Fig. 26—Resonant frequencies of a short-circuited slow-wave structure.

in the inset of Fig. 26, a perturbing object such as a small dielectric or metal sphere is moved along a predetermined line as, for example, the direction of propagation. Observations are made on the changes in resonant wavelength for which Slater [233] gives the relation

$$\frac{d\lambda}{\lambda} = -\frac{1}{2}\frac{\int_{\Delta V}(\mu_0 H^2 - \epsilon_0 E^2)dV}{\int_V (\mu_0 H^2 + \epsilon_0 E^2)dV} \tag{110}$$

where ΔV, V are, respectively, the perturbed and cavity volumes. The measurement is made absolute by determining the total stored energy by introducing [187] for, example, a small variable plunger in a region where H is zero and E constant. From knowledge of the phase velocity and field distribution, the coupling impedance may be calculated.

Helical Structures

Simple Helix

A widely-used slow-wave structure consists of a metallic conductor wound in the form of a helix with circular cross section. The propagation of electromagnetic waves on such helical structures was first studied by Pocklington [206] who assumed that there was a thin perfectly conducting wire. The solutions obtained predicted a travelling wave whose axial phase velocity is nearly c for low frequencies but reduces to $c \sin \psi_h$ for high frequencies. The latter result is equivalent to a wave with phase velocity c travelling along the wire. Under these circumstances it has been shown [138] that the wave possesses axial components of both electric and magnetic field and since it is evanescent over the wave front on the outside of the helix it may be regarded as an EH surface wave, *i.e.*, a mixture of TM and TE modes which contain roughly equal amounts of electric and magnetic energy. A pure EH wave may only exist as a travelling wave on a simple helix—two EH waves travelling in opposite directions result in an elliptically polarized EH surface wave whose plane of polarization rotates with position along the line.

Some basic properties emerge from the model applied by Ollendorf [188] and others [132], [150], [151], [202], in which the helix is replaced by an anisotropic sheet wound on a cylinder and conducting only in the ψ_h direction. This sheath model ignores the periodic structure of the actual helix as well as the finite size of the conductor. Sensiper [228] shows that solutions only exist for slow waves where $\beta > \beta_w$ and which represent modes characterized by different angular variations given by $e^{jm\theta}$. The usual $m=0$ wave shows large dispersion at low frequencies, but at higher frequencies, the phase and group velocities are nearly equal over a broad band. For modes where $m>1$ which occur when $2\pi r_h > \lambda$, the results are more complicated since there are now several waves per mode number. When these are plotted on an $\omega-\beta$ diagram it is observed that some branches have the phase and group velocities in opposite directions, corresponding with backward waves. The sheath model enables an estimate of the coupling impedance to be made but experiment [63] shows that this is about twice that possessed by practical structures.

The periodic nature of the helix is evident in analysis based on the tape model in which the conductor is considered to possess zero radial extent. The structures examined have included narrow tapes or wires [154], [155], [156], [197], [214], [215], [240], those with narrow gaps [266] and miscellaneous sections [49]. The developed tape helix [228] is shown in Fig. 27(a), practical structures having nearly equal gap and conductor widths. It is evident that

$$\cot \psi_h = 2\pi r_h / p. \tag{111}$$

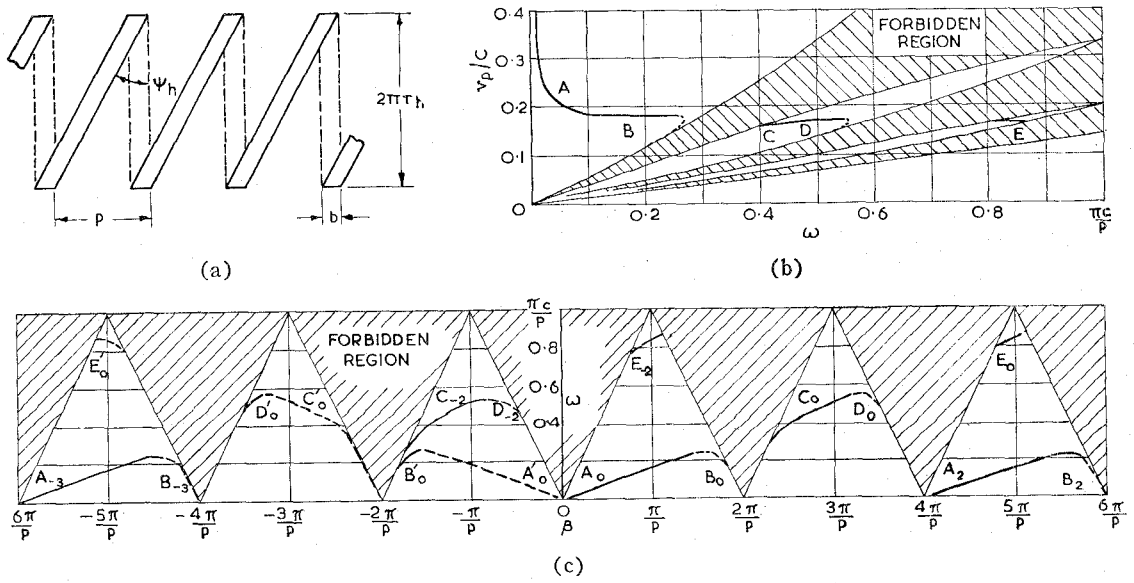

Fig. 27—Propagation along a tape helix. (a) Developed tape helix. (b) Phase velocity vs frequency. (c) Frequency characterisitc. Helix details are $\psi_h = 10°$, $\pi b/p = 0.1$.

The periodicity means that the wave function is characterized by a phase-change coefficient given by (1). Each angular mode of the helix now contains a complete set of space harmonics and, because of the close connection between translation and rotation in helical structures, the conditions for propagation require $m=n$. The exponential field relation then becomes

$$e^{-jn[(2\pi/p)z-\theta]}. \tag{112}$$

On applying the appropriate boundary conditions, analytical and graphical procedures give the results shown in Fig. 27(b) for the particular case of $\psi_h=10°$ and $\pi b/p=0.1$. The condition $\beta_n>\beta$ leads to the existence of forbidden regions which are associated [203] with coupling to fast waves [169] leading to radiation from the structure. No propagation takes place for the condition

$$\omega > \pi c/p \quad \text{or} \quad p < \tfrac{1}{2}\lambda. \tag{113}$$

The branches A to E correspond to different angular modes. If the helix is excited by a source at $z=0$, then for $z>0$ those waves with positive group velocity, indicated by full lines, can exist, whereas for $z<0$ those waves with negative group velocity, indicated by dotted lines, can occur.

For example, when $\omega<0.2\pi c/p$, propagation is possible with values of β_0 indicated by the branches A_0 and C_0 having positive phase velocities and B_0' having negative phase velocities. A few examples of the associated space harmonics marked with the appropriate subscript n, are also shown on the diagram; such harmonics have been observed experimentally [5], [280], [281]. The phase velocity [267] of the harmonics for various angular modes is given by

$$\frac{v_{pn}}{c}=\frac{\beta_w p/2\pi}{n+\beta_0 p/2\pi} \tag{114}$$

and values for various branches are given, as a function of ω, in Fig. 27(c). Eq. (114) shows, for example, that the first forward space harmonic is equivalent, as regards phase velocity, to the fundamental of a helix of radius $(2\pi r_h-\lambda)/2\pi$. Operation in such a harmonic allows [158] the use of a larger helix than with the usual fundamental mode.

Analysis of the power flow shows that a considerable fraction is carried by the space harmonics which explains the too-high coupling impedance given by the sheath-helix model. Butcher [38] extended his work on ladder lines to include calculation of the dispersion curves and coupling impedance of tape helices. Other studies of the helix have included power handling capacity [34] and attenuation [118], [222], [261]; the latter results have been extended [49] by the use of a correction factor to conductor shapes other than the thin tape.

Practical Modifications

Considerations arising in practical use require modification [161] of the simple helix. The effect of a dielectric has, for example, been examined [100] in the case of a spiral support for a coaxial line but most work [183], [189], [221], [240], [260] has been devoted to determining the change in characteristics of the metal helix in a continuous surround. In a comprehensive analysis, Tien [252] showed that the phase velocity and coupling impedance are reduced by a dielectric loading factor. This factor is typically 0.2–0.8 and can be raised by supporting the helix by tubes or wedges so that the main body of dielectric is away from the immediate vicinity of the helical surface.

Analysis with the sheath model suggests [251] that in certain circumstances small amounts of dielectric can reduce the dispersion of the helix. Experimental results of the attenuation of helices, both alone and in several types of dielectric support, have been quoted [196]. The frequency was in the range 2.6 to 3.6 kmc and the examined helices possesed diameters of 0.1 to 0.25 inch and wire to helix length ratios of 13 to 23. The helix attenuation was found to vary with the material, to increase linearly with frequency, and to have a flat maximum at a ratio of wire-diameter pitch of $\frac{1}{3}$. For a helix of 40 turns per inch with diameters 0.15-inch outside, 0.128-inch inside, the attenuation coefficients at 3 kmc for various materials and supports are given in Table I; the wire diameter was 0.011 inch. These results confirm that a fluted or similar support adds little to the helix losses.

TABLE I
ATTENUATION OF SUPPORTED HELICES

Type of Dielectric	Plain Tungsten Wire	Silver-Plated Tungsten Wire
	decibels per inch	decibels per inch
None	0.55	0.26
707 fluted glass tube	0.62	0.33
Quartz tube	0.75	0.42
707 plain glass tube	0.88	0.49

More complicated media which have been studied include attenuating layers [160], [284] and semiconductors [243]. Ferrites are of practical interest since the loss caused by this medium may be nonreciprocal in direction. Propagation along a helix surrounded by a ferrite sleeve has been analysed [250] in terms of a plane sheath model with nonreciprocal properties occurring under the condition of circumferential magnetization.

The properties of a helix with a coaxial inner conductor have been examined but the effect of an outer metallic sheath is more pronounced [8], [207], [229], [235], [283] since radiation from the helix is prevented. Under conditions of evanescent radial decay of the fields, the outer sheath has little effect unless it is very close or the frequency is low. For modes in which $v_p>c$ Stark [246] has shown that the fields have a radial dependence which oscillates outwards to the conducting

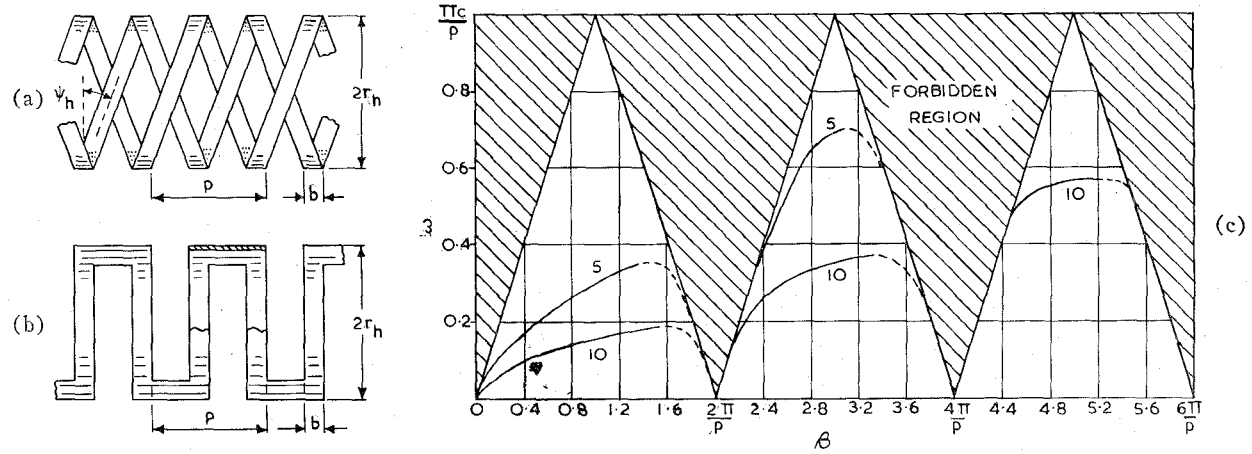

Fig. 28—Contra-wound helixes. (a) Twin tape helix. (b) Modified structure. (c) Frequency characteristic for helix with $2\pi b/p=1$ and cot ψ_h as parameter.

sheath in the manner noted in the case of capacitive loading of Fig. 4. In these "exceptional" regions the conditions resemble perturbed TE and TM modes of a coaxial line and circular waveguide.

If several helices each with the same pitch and radius are equally spaced in the axial direction, there results the multifilar helix [126], [238]. The curves of Fig. 27(b) still apply, but if N is the number of conductors the abscissa points $(-2\pi/p)$, 0, $(+2\pi p)$ and the ordinate point $\pi c/p$ are multiplied by N. According to the value of N, some of the space harmonic components will be missing.

The bifilar helix with $N=2$ has received much attention [86], [152], [175]. At low frequencies there is an extra mode present which is analogous to the TEM wave on a two-wire line. At any transverse plane the equal RF currents on the two tapes may thus be in-phase or out-of-phase. In the former case, odd space harmonics are zero and in Fig. 27(b) the solution corresponding to branch B_0 and the portion of branch C_0 along the forbidden boundary region disappear; the A_0 branch and the remaining portion of C_0 then join through the now-vanished forbidden region. In the out-of-phase case, the even space harmonics are zero. In either condition, the power carried by some of the unwanted components can be eliminated and a higher impedance for the desired modes is realized. The bifilar helix has received special study [280] regarding backward-wave per performance; in the push-pull mode it has substantially higher impedance [253] than the single helix.

As the pitch and diameter of a single helix are increased, the impedance of the fundamental is reduced [252], [253] while that of the $n=-1$ space harmonic is increased. Such an effect is undesirable in practice and may be eliminated by the contra-wound helix [46] which, as shown in Fig. 28(a), consists of two helices wound in opposite directions. An alternative version shown in Fig. 28(b) consists [25] of a spatial distortion which has the advantage of simplicity of construction. Single or multifilar helices are possible in both arrangements. Two modes, designated as the symmetric and antisymmetric, may be propagated and can be considered as arising from the combining of the single helix modes with different phases. In the former, the two modes are superimposed in phase and, in the latter, out of phase. In the symmetric mode, which is the one considered, the axial electric fields of the fundamental component add, and the resultant axial magnetic field, together with its associated stored energy, is zero. Thus the TE portion of the fundamental component is nonexistent so that the higher order space harmonics must have most of their energy in the magnetic or TE part of the field. This implies that the higher order space harmonics have small axial electric field components and, consequently, small impedance for backward waves.

The exponential term in the field equations now takes the form

$$\exp\{-j[(2\pi/p)(n+2n')z-m\theta]\}, \qquad (115)$$

where

$$\beta_{n,n'}=\beta_{0,0}+2\pi(n+2n')/p \qquad (116)$$

and is similar, if n' is omitted, to the single helix set of space harmonics. In Fig. 28(c), ω is plotted against β for two examples of twin helices with $2\pi b/p=1$, and cot $\psi_h=5$ and 10, respectively. The forbidden regions are the same as for the single helix, and the solution for cot $\psi_h=5$ has two branches, whereas that for cot $\psi_h=10$ has five, only three of which are shown. Measurements [25] on contra-wound helices show typically that there is an increase by a factor of 2 in the fundamental impedance and a reduction by a factor of 20 in the $n=-1$ space harmonic, as compared with the single helix. As expected from the diagrams, the phase velocities show increased dispersion over the single helix.

Numerous practical designs of helices have been developed [71], [84] for use at microwave frequencies. A typical example of 0.048-inch diameter copper wire, diameter of turn 0.25-inch and pitch 0.157-inch would have an axial velocity of 0.1 c, attenuation, 2 decibels per meter, and coupling impedance, 500 ohms. The ap-

plications of helices require measurement [184] of their essential properties and the design of broad-band transitions from coaxial and waveguide transmission lines. In experiments [282] on such devices, mercury formed a convenient and efficient moveable short circuit. Transitions from coaxial line [170], [287] may be via the inner conductor, the outer being continued for a short distance as a sheath surrounding the helix. The reflections caused by changes in pitch angle [200] are also relevant.

Coupling of power into and out of a helix at any particular point can be achieved [59] with an additional surrounding concentric helix. The coupling is strong when the helices have very nearly equal velocities of propagation when uncoupled and they are wound in opposite senses. These transitions resemble directional couplers, and modifications such as tapering or stepping can be employed. Complete power transfer can be affected over a distance of the order of one-helix wavelength (about 0.1λ). Coupled helices have no direct connection and thus the input or output circuit may be external to the device containing the main helix. The coupling conditions are modified in the presence of a dielectric or electron beam [272] and triangular as well as semicircular-re-entrant coupling helices have been developed [10]. A typical [166] helix coupler for frequencies of 1.7–2.3 kmc possessed a diameter ratio of 2.7 with an input VSWR of 1.3 and a directivity of 4 db. Such large diameter ratios lead to difficulty in matching and thus a third helix, intermediately placed and unconnected but contra-wound with respect to the other two, has been proposed and tested [180].

A helical structure may be made by spiralling [113] a rectangular waveguide. Such an arrangement has been analysed [274], [275] by considering a guide whose axis is uniformly curved and adopting the fiction that points at angular separation of 2π are not equivalent but differ in axial position by the pitch. If the rectangular guide propagating its dominant mode is orientated with its major dimension perpendicular to the axis of the structure, a TM_{01} mode is supported whereas the orthogonal orientation supports a TE_{01} mode. Such a structure is very dispersive [52] if coiled, for example, with a radius ratio of 5:1. Improvement results when there is coupling between turns as, for instance, in the extreme case of a coaxial line with helical grooves in one or both conductors. The properties now resemble those of the stub-loaded line provided that account is taken of circumferential as well as of axial propagation. A further modification entails the removal of the center conductor to form an open helical waveguide which has a low frequency cutoff.

Acknowledgment

The author is grateful to G. J. Rich, Dr. H. W. Duckworth, Dr. P. N. Butcher, Dr. A. E. Karbowiak and Prof. A. L. Cullen for helpful comments on the manuscript.

Bibliography

[1] M. Abele, "Theory of the Propagation of Electromagnetic Waves along a Dielectric Guide of Circular Section," Consiglo Nazionale Delle Richerche, Tipographia Del Senato, Rome, Italy; 1948.
[2] R. B. Adler, "Waves on inhomogenous cylindrical structures," Proc. IRE, vol. 40, pp. 339–348; March, 1952.
[3] A. W. Aikin, "Measurements in travelling-wave structures," *Wireless Engr.*, vol. 32, p. 230; 1955.
[4] A. I. Akhiezer, and Y. B. Faynberg, "Slow electromagnetic waves," *Uspekhi Fiz. Nauk*, vol. 44, p. 321;1951.
[5] C. P. Allen and G. M. Clarke, "Interpretation of wavelength measurements on tape helices," *Proc. IEE*, vol. 103, pt. C, pp. 171–176; March, 1956.
[6] C. M. Angulo, "Diffraction of surface waves by a semi-infinite slab," IRE Trans. on Antennas and Propagation, vol. AP-5, pp. 100–109; January, 1957.
[7] C. M. Angulo and W. S. C. Chang, "The excitation of a dielectric rod by a cylindrical waveguide," IRE Trans. on Microwave Theory and Techniques, vol. MTT-6, pp. 389–393; October, 1958.
[8] E. V. Anisimov and N. M. Sovetov, "The propagation of electromagnetic waves along a helical strip in a circular waveguide," *Zhur. Tekh.*, vol. 25, p. 1965; 1955.
[9] T. Ankel, "Investigation of the propagation of signals in dispersive media, using an acoustic model," *Z. Physik*, vol. 144, p. 120; 1956.
[10] E. A. Ash and J. D. Pattenden, "Modified transmission-line couplers for helice," *Proc. IEE*, vol. 105, pt. B, pp. 762–768; May, 1958.
[11] E. A. Ash, " A new type of slow-wave structure for millimetric wavelengths," *Proc. IEE*, vol. 105, pt. B, pp. 737–745; May, 1958.
[12] S. S. Attwood, "Surface-wave propagation over a coated plane conductor," *J. Appl. Phys.*, vol. 22, pp. 504–509; April, 1951.
[13] H. Awender and O. Lange, "The propagation of decimetre and centimetre waves along single metallic and dielectric wires," *Funktech. Monatshefte*, pt. 2, p. 5, 51; 1938.
[14] H. E. M. Barlow and A. E. Karbowiak, "An investigation of the characteristics of cylindrical surface waves," *Proc. IEE*, vol. 100, pt. III, pp. 321–328; November, 1953.
[15] H. E. M. Barlow and A. L. Cullen, "Surface waves," *Proc. IEE*, vol. 100, pt. III, pp. 329–347; November, 1953.
[16] H. E. M. Barlow and A. E. Karbowiak, "Proposed use of a cylindrical surface-wave resonator for the determination of the velocity of short electro-magnetic waves," *Brit. J. App. Phys.*, vol. 4, pp. 186–187; June, 1953.
[17] H. E. M. Barlow and A. E. Karbowiak, "An experimental investigation of the properties of corrugated cylindrical surface waveguides," *Proc. IEE*, vol. 101, pt. III, pp. 182–188; May, 1954.
[18] H. E. M. Barlow and A. E. Karbowiak, "An experimental investigation of axial cylindrical surface waves supported by capacitive surfaces," *Proc. IEE*, vol. 102, pt. B, pp. 313–322; May, 1955.
[19] H. E. M. Barlow, "The power radiated by a surface wave circulating around a cylindrical surface," *Proc. IEE*, vol. 106, pt. B, pp. 180–185; March, 1959.
[20] H. E. M. Barlow, "Surface waves," Proc. IRE, vol. 46, pp. 1413–1417; July, 1958.
[21] E. Belohoubek, "Propagation characteristics of slow-wave structures derived from coupled resonators," *RCA Rev.*, vol. 19, p. 283; 1958.
[22] T. Berceli, "Surface-wave propagation along coated wires," *Acta Tech. Acad. Science Hungaricae*, vol. 17, p. 269; 1957.
[23] F. Bertein and W. Chahid, "Production of slow electromagnetic waves by means of cylindrical current sheets," *Compt. Rend. Acad. Sci. (Paris)*, vol. 242, p. 2918; 1956.
[24] V. I. Bespalov and A. B. Gapanov, "Influence of inhomogeneities on the propagation of electromagnetic waves in periodic structures," *Radiotekh. i Elektron.*, vol. 1, p. 772; 1956.
[25] C. K. Birdsall and T. E. Everhart, "Modified contra-wound helix circuits for high power travelling wave tubers," IRE Trans. on Electron Devices, vol. ED-3, pp. 190–204; October, 1956.
[26] F. E. Borgnis, "Electric waves on delay lines," *Elektrotech. Z.*, vol. 79A, p. 383; 1958.
[27] F. E. Borgnis and C. H. Papas, "Electromagnetic waveguides," in "Encyclopedia of Physics," vol. 16; Springer-Verlag, Berlin, Ger.; 1958.
[28] D. B. Brick, "The radiation of a hertzian dipole over a coated conductor," *Proc. IEE*, vol. 120, pt. C, pp. 104–121; March, 1955.

[29] D. B. Brick, "The excitation of surface waves by a vertical antenna," PROC. IRE, vol. 43, pp. 221–727; June, 1955.
[30] L. Brillouin, "Wave Propagation in Periodic Structures," McGraw-Hill Book Co., Inc., New York, N. Y.; 1946.
[31] L. Brillouin, "Wave guides for slow waves," *J. Appl. Phys.*, vol. 19, p. 1023; 1948.
[32] J. Brown, "The types of waves which may exist near a guiding surface," *Proc. IEE*, vol. 100, pt. III, pp. 363–364; November, 1953.
[33] J. Brown and K. P. Sharma, "The launching of radial cylindrical surface waves by a circumferential slot," *Proc. IEE*, vol. 106, pt. B, pp. 123–128; March, 1959.
[34] J. H. Bryant and E. F. White, "Attenuation and power-handling capability of helical radio-frequency lines," IRE TRANS. ON MICROWAVE THEORY AND TECHNIQUES, vol. MTT-1, pp. 33–38; November, 1953.
[35] J. H. Bryant, "Some wave properties of helical conductors," *Elec. Commun.*, vol. 631, p. 50; 1954.
[36] P. N. Butcher, "A new treatment of lossy periodic waveguides," *Proc. IEE*, vol. 103, pt. B, pp. 301–306; May, 1956.
[37] P. N. Butcher, "A theoretical study of propagation along tape ladder lines," *Proc. IEE*, vol. 104, pt. B, pp. 169–176; March, 1957.
[38] P. N. Butcher, "The coupling impedance of tape structures," *Proc. IEE*, vol. 104, pt. B, pp. 177–187; March, 1957.
[39] G. A. Campbell, "On loaded lines in telephonic transmission," *Phil. Mag.*, vol. 5, p. 319; 1903.
[40] J. R. Carson, S. P. Mead, and S. A. Schelkunoff, "Hyperfrequency waveguides—mathematical theory," *Bell Sys. Tech. J.*, vol. 15, p. 310; 1936.
[41] C. H. Chandler, "An investigation of dielectric rod as wave guide," *J. Appl. Phys.*, vol. 20, pp. 1188–1192; December, 1949.
[42] S. K. Chatterjee and P. Madhaven, "Propagation of microwaves on a single wire," *J. Indian Inst. Sci.*, vol. 37 B, p. 200; 1955.
[43] S. K. Chatterjee and R. Chatterjee, "Propagation of microwave along a solid conductor embedded in three coaxial dielectrics," *J. Indian Inst. Sci.*, vol. 38 B, p. 157, 1956; vol. 39 B, p. 7, 1957.
[44] S. K. Chatterjee and R. Chatterjee, "Surface waveguides," *J. Inst. Telecommun. Engrs. (India)*, vol. 4, p. 90; 1958.
[45] P. Chavance and B. Chiron, "Experimental study of the transmission of centimetre waves along wire waveguides," *Ann. Télécommun.*, vol. 8, p. 367; 1953.
[46] M. Chodorow and E. L. Chu, "Cross-wound twin helices for traveling-wave tubes," *J. Appl. Phys.*, vol. 26, p. 33; January, 1955.
[47] M. Chodorow and R. A. Craig, "Some new circuits for high-power traveling wave tubes," PROC. IRE, vol. 45, pp. 1106–1118; August, 1957.
[48] M. Chodorow and E. J. Nalos, "The design of high-power traveling-wave tubes," PROC. IRE, vol. 44, pp. 649–659; May, 1956.
[49] C. M. Chu, "Propagation of waves in helical wave guides," *J. Appl. Phys.*, vol. 29, pp. 88–99; January, 1958.
[50] E. L. Chu and W. W. Hansen, "The theory of disk-loaded waveguides," *J. Appl. Phys.*, vol. 18, pp. 996; 1947.
[51] E. L. Chu and W. W. Hansen, "Disk loaded waveguides," *J. Appl. Phys.*, vol. 20, p. 280; 1949.
[52] G. M. Clarke, "Helical waveguides—closed, open and coaxial," *J. Brit. IRE*, vol. 18, pp. 359–361; June, 1958.
[53] A. G. Clavier and V. Altovsky, "Experimental researches on the propagation of electromagnetic waves in dielectric guides," *Elec. Commun.*, vol. 18, p. 8; 1940.
[54] P. J. M. Clavier, "Physical explanation of the surface wave on a dielectric-coated line," *Cables & Transmission*, vol. 7, p. 34; 1953.
[55] J. F. Colin, "Propagation of an electromagnetic wave guided by a metal surface with dielectric coating," *L'Onde Electrique*, vol. 31, p. 245; 1951.
[56] R. Combe, "Pass band and dispersion of waveguides loaded with circular irises," *Compt. Rend. Acad. Sci. (Paris)*, vol. 238, p. 1697; 1954.
[57] R. Combe, "Attenuation coefficient of waveguides loaded with circular irises," *Compt. Rend. Acad. Sci. (Paris)*, vol. 238, p. 2063; 1954.
[58] S. N. Contractor and S. K. Chatterjee, "Propagation of microwaves on a single wire: part 2," *J. Indian Inst. Sci.*, vol. 39 B, p. 52; 1957.
[59] J. S. Cook, R. Kompfner, and C. F. Quate, "Coupled helices," *Bell Sys. Tech. J.*, vol. 35, pp. 127–178; January, 1956.
[60] A. L. Cullen, "Waveguide field patterns in evanescent modes," *Wireless Engr.*, vol. 26, p. 317; 1949.
[61] A. L. Cullen, "The excitation of plane surface waves," *Proc. IEE*, vol. 191, pt. IV, p. 225; 1954.
[62] A. L. Cullen, "A Note on the excitation of surface waves," *Proc. IEE*, vol. 104, pt. C, pp. 472–474; September, 1957.
[63] C. C. Cutler, "Experimental determination of helical-wave properties," PROC. IRE, vol. 36, pp. 230–233; February, 1948.
[64] C. C. Cutler, "Electromagnetic Waves Guided by Corrugated Conducting Surfaces," Bell Telephone Labs., New York, N. Y., unpublished rept.; October, 1944.
[65] J. Dain, "Some fundamental aspects of slow wave propagation," *L'Onde Électrique*, vol. 37, p. 86; 1957.
[66] J. Dain, "The propagation of slow waves," *Electronic Engrg.*, vol. 30, pp. 388–393; June, 1958.
[67] W. Dallenback, "Travelling waves between two parallel diaphragm-loaded reflector planes," *Arch. elek. Übertragung*, vol. 7, p. 297; 1953.
[68] R. W. DeGrasse, "Slow-wave structures for unilateral solid-state maser amplifiers," 1958 WESCON CONVENTION RECORD, pt. 3, pp. 29–35.
[69] H. Derfler, "On the theory of disc-loaded waveguide," *Z. Ange. Math. Phys.*, vol. 6, p. 190; 1955.
[70] C. C. Dewey, P. Parzen, and T. M. Marchese, "Periodic waveguide travelling-wave amplifier for medium powers," PROC. IRE, vol. 39, pp. 153–159; February, 1951.
[71] W. J. Dodds and R. W. Peter, "Filter helix travelling-wave-tube," *RCA Rev.*, vol. 14, p. 502; 1953.
[72] L. Drozdowicz, "Guiding of an electromagnetic wave by a single conductor," *Przeglad Telekomun.*, vol. 1, p. 1; 1953.
[73] R. H. DuHamel and J. W. Duncan, "Launching efficiency of wires and slots for a dielectric rod waveguide," IRE TRANS. ON MICROWAVE THEORY AND TECHNIQUES, vol. MTT-6, pp. 277–284; July, 1958.
[74] R. B. Dyott, "The launching of electromagnetic waves on a cylindrical conductor," *Proc. IEE*, vol. 99, pt. III, pp. 408–413; November, 1952.
[75] H. Ehrenspeck, W. Gerbes, and F. J. Zucker, "Trapped wave antennas," 1954 IRE CONVENTION RECORD, pt. 1, pp. 25–30.
[76] R. S. Elliott, "On the theory of corrugated plane surfaces," IRE TRANS. ON ANTENNAS AND PROPAGATION, vol. AP-2, pp. 71–81; April, 1954.
[77] R. S. Elliott, "Azimuthal surface waves on circular cylinders," *J. Appl. Phys.*, vol. 26, pp. 368–376; April, 1955.
[78] W. M. Elsasser, "Attenuation in a dielectric circular rod," *J. Appl. Phys.*, vol. 20, pp. 1193–1196; December, 1949.
[79] B. Epsztein and G. Mourier, "Definition, measurement and character of the phase velocities in systems with periodic structure," *Ann. Radioelectricité*, vol. 10, p. 64; 1955.
[80] Y. N. Fel'd, "Infinite systems of linear algebraic equations connected with problems of semi-infinite periodic structures," *Compt. Rend. Acad. Sci. U.R.S.S.*, vol. 102, p. 257; 1955.
[81] W. M. G. Fernando and H. E. M. Barlow, "An investigation of the properties of radial cylindrical surface waves launched over flat reactive surfaces," *Proc. IEE*, vol. 103, pt. B, pp. 307–318; May, 1956.
[82] L. M. Field, "Some slow-wave structures for travelling wave tubes," PROC. IRE, vol. 37, pp. 34–40; January, 1949.
[83] L. M. Field, "Recent developments in traveling-wave valves," *Electronics*, p. 150; January, 1950.
[84] R. C. Fletcher, "Helix parameters used in travelling-wave tube theory," PROC. IRE, vol. 38, pp. 413–417; April, 1950.
[85] R. C. Fletcher, "A broad-band interdigital circuit for use in travelling-wave-type amplifiers," PROC. IRE, vol. 40, pp. 951–958; August, 1952.
[86] V. J. Fowler, "Analysis of helical transmission lines by means of the complete circuit equations," IRE TRANS. ON ANTENNAS AND PROPAGATION, vol. AP-2, pp. 132–143; October, 1954.
[87] B. Friedman, and W. E. Williams, "Excitation of surface waves," *Proc. IEE*, vol. 105, pt. C, pp. 252–258; March, 1958.
[88] C. Froese, and J. R. Wait, "Calculated diffraction patterns of dielectric rods at centimetre wavelengths," *Canad. J. Phys.*, vol. 32, p. 775; 1954.
[89] A. Fromageot, and B. Louis, "Propagation of electromagnetic waves along a conducting wire with thin dielectric covering," *Bull Soc. Franç., Electriciens*, vol. 1, p. 291; 1951.
[90] M. A. Gintsburg, "Surface waves on the boundary of a gyrotropic medium," *Zhur. Eksp. i Teoret. Fiz.*, vol. 34, p. 1635; 1958.
[91] J. F. Gittins, N. H. Rock, and A. B. J. Sullivan, "An experimental high-power pulsed travelling-wave tube," *J. Electronics and Control*, vol. 3, p. 267; 1957.
[92] G. Goubau, "Designing surface-wave transmission lines," *Electronics*, vol. 27, pp. 180–184; April, 1954.
[93] G. Goubau, "On the Zenneck surface wave," *Z. Angew. Phys.*, vol. 3, p. 103; 1951.
[94] G. Goubau, "Surface waves and their application to transmission lines," *J. Appl. Phys.*, vol. 21, pp. 1119–1128; November, 1950.

[95] G. Goubau, "Surface-wave transmission line," *Radio and TV News*, vol. 14, p. 10; 1950.
[96] G. Goubau, "On the excitation of surface waves," PROC. IRE, vol. 40, pp. 865–868; July, 1952.
[97] G. Goubau, "Single-conductor surface-wave transmission lines," PROC. IRE, vol. 39, pp. 619–624; June, 1951.
[98] G. Goubau, "Open wire lines," IRE TRANS. ON MICROWAVE THEORY AND TECHNIQUES, vol. MTT-4, pp. 197–200; October, 1956.
[99] A. C. Grace and J. A. Lane, "Surface-wave transmission lines," *Wireless Engr.*, vol. 29, p. 230; 1952.
[100] J. W. E. Griemsmann, "An approximate analysis of coaxial line with a helical dielectric support," IRE TRANS. ON MICROWAVE THEORY AND TECHNIQUES, vol. MTT-4, pp. 13–23; January, 1956.
[101] C. C. Grosjean, "Theory of circularly symmetric standing TM waves in terminated iris-loaded waveguides," *Nuovo Cim.*, vol. 2, p. 11; 1955.
[102] C. C. Grosjean, "Transformation of a frequency equation in corrugated waveguide theory," *Nuovo Cim.*, vol. 1, p. 174; 1955.
[103] C. C. Grosjean and V. J. Vanhuyse, "Experimental verification of a frequency equation for corrugated waveguides," *Nuovo Cim.*, vol. 1, p. 193; 1955.
[104] C. C. Grosjean, "Mathematical transformation of a system of equations appearing in the theory of TM wave propagation in corrugated guides," *Nuovo Cim.*, vol. 1, p. 439; 1955.
[105] C. C. Grosjean, "Note on the properties of two functions appearing in the theory of TM wave propagation through periodically iris-loaded guides," *Nuovo Cim.*, vol. 1, p. 1264; 1955.
[106] P. Guénard, O. Doehler, and R. Warnecke, "Properties of lines with periodic structures," *Compt. Rend. Acad. Sci. (Paris)*, vol. 235, p. 32; 1952.
[107] W. Gunn, "Application possibilities of a surface-wave mode," *Marconi Rev.*, vol. 15, p. 145; 1952.
[108] R. C. Hansen, "Single-slab arbitrary-polarization surface-wave structure," IRE TRANS. ON MICROWAVE THEORY AND TECHNIQUES, vol. MTT-5, pp. 115–120; April, 1957.
[109] F. Harms, "Electromagnetic waves on a wire with a cylindrical insulating sheath," *Ann. Phys.*, vol. 23, p. 44; 1907.
[110] A. F. Harvey, "Radio-frequency aspects of electro-nuclear accelerators," *Proc. IEE*, vol. 106, pt. B, pp. 43–57; January, 1959.
[111] L. Hatkin, "Analysis of propagating modes in dielectric sheets," PROC. IRE, vol. 42, pp. 1565–1568; October, 1954.
[112] J. Hirano, "Characteristics of interdigital circuits and their use for amplifiers," *Proc. IEE*, vol. 105, pt. B, pp. 780–785; May, 1958.
[113] B. T. Henoch, "Investigations of the disk-loaded and helical waveguide," *Kgl. Tek. Högskol. Handl.*, no. 129, p. 1; 1958.
[114] G. Hok, "Calculation of a waveguide loaded resonator for interdigital magnetrons," PROC. IRE, vol. 41, pp. 763–769; June, 1953.
[115] A. Hondros and P. Debye, "Electromagnetic waves in dielectric wires," *Ann. Physik*, vol. 32, p. 465; 1910.
[116] D. Hondros, "Electromagnetic waves on wires," *Ann. Physik*, vol. 30, p. 905; 1909.
[117] K. Horiuchi, "Surface-wave propagation over a coated conductor with small cylindrical curvature in direction of travel," *J. Appl. Phys.*, vol. 24, p. 961; 1953.
[118] T. Hosono, "Radio-wave propagation along a helix," *J. Inst. Elec. Commun. Engrs. (Japan)*, vol. 38, p. 34; 1955.
[119] K. Hübener, "Investigations on helical lines," *Nachrichtentech. Zeitung*, vol. 9, p. 581; 1956.
[120] J. F. Hull, G. Novick and B. D. Kumpfer, "A high-power delay line for a travelling-wave amplifier or oscillator," *Proc. NEC*, vol. 8, p. 313; 1952.
[121] R. A. Hurd, "The propagation of an electro-magnetic wave along an infinite corrugated surface," *Can. J. Phys.*, vol. 32, p. 727; 1954.
[122] R. A. Hurd, "Surface Waves on a Two-Layer Dielectric-Coated Wire," Natl. Res. Council of Canada, Ottawa, Ont., Publication No. 3187, p. 1; 1953.
[123] C. Jauquet, "Excitation of a transverse magnetic surface-wave propagated on a dielectric cylinder," *Ann. Télécommun.*, vol. 12, p. 217; 1957.
[124] E. T. Jaynes, "The concept and measurement of impedance in periodically loaded wave guides," *J. Appl. Phys.*, vol. 23, p. 1077; 1952.
[125] M. Jessel and R. Wallauschek, "Experimental study of propagation along a delay line in the form of a helix," *Ann. Télécommun.*, vol. 3, p. 291; 1948.
[126] H. R. Johnson, T. E. Everhart, and A. E. Siegman, "Wave propagation on multifilar helices," IRE TRANS. ON ELECTRON DEVICES, vol. ED-3, pp. 18–24; January, 1956.
[127] C. E. Jordan and A. B. McLay, "Diffraction of 3.2 cm electromagnetic waves by dielectric rods: part 3—lucite 1½ in.—diameter semicylinder, fields very close to surfaces," *Can. J. Phys.*, vol. 35, p. 1253; 1957.
[128] C. Jouget, "The surface wave on a dielectric cylinder: the method of launching it and its characteristics," *Rev. HF (Brussels)*, vol. 3, p. 283; 1956.
[128a] C. Jouget, "Excitation of a transverse magnetic surface wave propagated on a dielectric cylinder," *Ann. Télécommun.*, vol. 12, p. 217; 1957.
[129] M. Jouget, "Propagation in a dielectric transmission line," *Compt. Rend. Acad. Sci. (Paris)*, vol. 237, p. 1656; 1953.
[130] M. Jouget, "Waveguides with discontinuous structure," *Compt. Rend. Acad. Sci. (Paris)*, vol. 245, p. 297; 1957.
[131] H. Kaden, "Advances in the theory of waves on wires," *Arch. elek. Übertragung*, vol. 5, p. 399; 1951.
[132] Kaden, H. "A general theory of the helical line," *Arch. elek. Übertragung*, vol. 5, p. 534; 1951.
[133] H. Kaden, "Dielectric and metal waveguides," *Arch. elek. Übertragung*, vol. 6, p. 319; 1952.
[134] H. Kaden, "Recent research on the transmission of signals along metal and dielectric lines," *Fernmeldetech. Z.*, vol. 6, p. 432; 1953.
[135] K. Kamirijo, H. Hozumi, Y. Shibata, and Y. Fukushima, "Measurements of field patterns for a comb-type slow-wave structure," *Proc. IEE*, vol. 105, pt. B, pp. 890–892; May, 1958.
[136] M. D. Karasev and V. A. Apanasenko, "Surface waves propagated along a single cylindrical conductor," *Zhur. Tekh. Fiz.*, vol. 24, p. 662; 1954.
[137] A. E. Karbowiak, "Theory of composite guides: stratified guides for surface waves," *Proc. IEE*, vol. 101, pt. III, pp. 238–242; July, 1954.
[138] A. E. Karbowiak, "The E-H surface wave," *Wireless Engr.*, vol. 31, p. 71; 1954.
[139] A. E. Karbowiak, "The elliptic surface wave," *Brit. J. Appl. Phys.*, vol. 5, pp. 328–335; September, 1954.
[140] A. E. Karbowiak, "On the surface impedance of a corrugated waveguide," *Proc. IEE*, vol. 102, pt. B, pp. 501–502; July, 1955.
[141] A. E. Karbowiak, "Microwave propagation in anisotropic waveguides," *Proc. IEE*, vol. 103, pt. 3, pp. 139–144; March, 1956.
[142] H. Kaufman, "Bibliography of nonuniform transmission lines," IRE TRANS. ON ANTENNAS AND PROPAGATION, vol. AP-3, pp. 218–220; October, 1955.
[143] A. F. Kay and F. J. Zucker, "Efficiency of surface wave excitation," 1955 IRE CONVENTION RECORD, pt. 1, pp. 1–5.
[144] E. Kettel, "A waveguide with phase velocity $v<c$ for the E_{10}-wave," *Frequenz*, vol. 3, pp. 73–00; Month, 1949.
[145] D. G. Kiely, "Experiments with single-wire transmission lines at 3 cm wavelength," *J. Brit. IRE*, vol. 13, pp. 194–199; April, 1953.
[146] D. D. King, "Dielectric image line," *J. Appl. Phys.*, vol. 23, pp. 699–700; June, 1952.
[147] D. D. King, "Properties of dielectric image lines," IRE TRANS. ON MICROWAVE THEORY AND TECHNIQUES, vol. MTT-3, pp. 75–81; March, 1955.
[148] D. D. King, "Circuit components in dielectric image lines," IRE TRANS. ON MICROWAVE THEORY AND TECHNIQUES, vol. MTT-3, pp. 35–39; December, 1955.
[149] D. D. King and S. P. Schlesinger, "Losses in dielectric image lines," IRE TRANS. ON MICROWAVE THEORY AND TECHNIQUES, vol. MTT-5, pp. 31–35; January, 1957.
[149a] H. S. Kirschbaurn and R. Tsu, "A study of a serrated ridge waveguide," IRE TRANS. ON MICROWAVE THEORY AND TECHNIQUES, vol. MTT-7, pp. 142–148; January, 1959.
[150] W. Klein, "The delay line as a component of valves," *Arch. Elektrotech.*, vol. 40, p. 280; 1952.
[151] W. Klein, "The dimensions of helices in travelling wave tubes," *Arch. elek. Übertragung*, vol. 10, p. 261; 1956.
[152] H. Kleinwachter and H. Weiss, "Bifilar line with large flexibility and rapid diminution of radial field for the transmission of hyperfrequencies," *L'Onde Électrique*, vol. 32, p. 46; 1952.
[153] A. Klemt, "Contribution to the propagation of electromagnetic waves along dielectric wires," *Funktech. Monatshefte*, vol. 4, p. 122; 1939.
[154] S. K. Kogan, "The propagation of waves along an endless helix," *Compt. Rend. Acad. Sci. U.R.S.S.*, vol. 66, p. 867; 1949.
[155] S. K. Kogan, "The excitation of a helical conductor," *Compt. Rend. Acad. Sci. U.R.S.S.*, vol. 74, p. 487; 1950.
[156] S. K. Kogan, "Theory of helical lines," *Compt Rend. Acad. Sci. U.R.S.S.*, vol. 107, p. 541; 1956.

[157] E. T. Kornhauser, "Propagation on dielectric coated wires," *J. Appl. Phys.*, vol. 22, p. 525; April, 1951.
[158] J. Koyama, "An application of the spatial-harmonic wave on a large-diameter helix," *Proc. IEE*, vol. 105, pt. B, pp. 412–414; May, 1958.
[159] R. L. Kyhl, "The use of non-Euclidean geometry in measurements of periodically loaded transmission lines," IRE TRANS. ON MICROWAVE THEORY AND TECHNIQUE, vol. MTT-4, pp. 111–115; April, 1956.
[160] G. Landauer, "The helical line with a coaxial cylindrical attenuating layer," *Arch. elek. Übertragung*, vol. 11, p. 267; 1957.
[161] P. Lapostalle, "Helices for travelling-wave valves: effect of supports, attenuation: parasitic modes," *Ann. Télécommun.*, vol. 12, p. 34; 1957.
[162] J. D. Lawson, "A method of launching surface waves," PROC. IRE, vol. 44, p. 111; January, 1956.
[163] A. Leblond and G. Mourier, "Investigation of lines with periodic bar structure for VHF valves: parts 1 and 2," *Ann. Radioélectricité*, vol. 9, pp. 180, 311; 1954.
[164] A. Leblond, "Investigation of an interdigital line operating in the vicinity of the π mode," *Ann. Radioélectricité*, vol. 10, p. 83; 1955.
[165] J. Levy, "Transmission of electromagnetic guided waves through a series of symmetrical and equidistant obstacles," *Câbles & Transmission*, vol. 1, p. 103; 1947.
[166] P. A. Lindsay and K. D. Collins, "Some aspects of the design of a helical coupler for a travelling-wave tube operating in the 2Gc/s band," *Proc. IEE*, vol. 105, pt. B, pp. 756–761; May, 1958.
[167] A. W. Lines, G. R. Nicoll, and A. M. Woodward, "Some properties of waveguides with periodic structures," *Proc. IEE*, vol. 97, pt. III, pp. 263–276; July, 1950.
[168] Y. T. Lo, "Electromagnetic field of a dipole source above a grounded dielectric slab," *J. Appl. Phys.*, vol. 25, pp. 733–740; July, 1954.
[169] L. N. Loshakov and E. B. Ol'derogge, "Fast waves in a coaxial helical line," *Radiotekhnika*, vol. 12, p. 25; 1957.
[170] C. O. Lund, "Broadband transition from coaxial line to helix," *RCA Rev.*, vol. 11, p. 133; 1950.
[171] P. Mallach, "Investigations on dielectric waveguides in rod or tube form," *Fernmeldetech. Z.*, vol. 8, p. 8; 1955.
[172] D. Marcuse, "A new type of surface waveguide with bandpass properties," *Arch. elek. Übertragung*, vol. 11, p. 146; 1957.
[173] D. Marcuse, "Investigation of the energy exchange and the field distribution for parallel surface-wave transmission lines," *Arch. elek. Übertragung*, vol. 10, p. 117; 1956.
[174] A. A. Meyerhoff, "Interaction between surface-wave transmission lines," PROC. IRE, vol. 40, pp. 1061–1065; September, 1952.
[175] V. S. Mikhalevski, "Theory of twin-helix coaxial line," *Radiotekh. i Elektron.*, vol. 1, p. 1309; 1956.
[176] M. A. Miller, "Propagation of electromagnetic waves over plane surface with anisotropic homogeneous boundary conditions," *Compt. Rend. Acad. Sci. U.R.S.S.*, vol. 87, p. 511; 1952.
[177] M. A. Miller, "Elektromagnetic surface waves in rectangular channels," *Zhur. Tekh. Fiz.*, vol. 25, p. 1972; 1955.
[178] M. A. Miller and V. I. Tolanov, "Electromagnetic surface waves, guided by a boundary with small curvature," *Zhur. Tekh. Fiz.*, vol. 26, p. 2755; 1956.
[179] S. Millman, "A spatial-harmonic travelling-wave amplifier for six-millimeters wavelength," PROC. IRE, vol. 39, pp. 1035–1943; September, 1951.
[180] B. Minakovic, "The coupling of three coaxial helices," *Proc. IEE*, vol. 105, pt. B, pp. 769–778; May, 1958.
[181] R. G. Mirimahov and G. I. Zhileiko, "A new type of waveguide with diaphragms," *Radiotekh. i Elektron.*, vol. 1, p. 1374; 1956.
[181a] R. A. Moore and R. E. Beam, "A duo-dielectric parallel-plane waveguide," *Proc. NEC*, vol. 12, p. 689; 1956.
[182] G. Mourier, "Bi-dimensional and Tri-dimensional periodic structure circuits," *L'Onde Électrique*, vol. 37, p. 86; 1957.
[183] M. Muller, "Dielectric in the field of helical lines," *Die Telefunken-Rohre*, no. 4, p. 100; 1953.
[184] R. Müller, "Measurement of the coupling impedances of delay lines," *Arch. elek. Übertragung*, vol. 10, p. 424; 1956.
[185] R. Müller, "Reflection of electromagnetic waves at inhomogeneous boundary surfaces with a periodic structure perpendicular to the electric vector," *Arch. elek. Übertragung*, vol. 7, p. 492; 1953.
[186] L. B. Mullett and B. G. Loach, "Waveguide systems with negative phase velocities," *Nature*, vol. 169, p. 1011; 1952.
[187] E. J. Nalos, "Measurement of circuit impedance of periodically loaded structures by frequency perturbation," PROC. IRE, vol. 42, pp. 1508–1511; October, 1954.
[188] F. Ollendorf, "The Theoretical Foundations of High-Frequency Technique," Springer-Verlag, Berlin, Ger.; 1926.
[189] S. Olving, "Electromagnetic wave propagation on helical conductors embedded in dielectric medium," *Chalmers Tek. Högskol. Handl.*, no. 156, p. 1; 1955.
[190] H. Ott, "Surface waves," *Arch. elek. Übertragung*, vol. 5, p. 343; 1951.
[191] P. Palluel and J. Arnaud, "Results on delay lines for high-power travelling-wave tubes," *Proc. IEE*, vol. 105, pt. B, p. 727; May, 1958.
[192] F. Paschke, "Investigation of an interdigital delay line," *Arch. elekt. Übertragung*, vol. 10, p. 195; 1956.
[193] F. Paschke, "A note on the dispersion of interdigital delay lines," *RCA Rev.*, vol. 19, p. 418; 1958.
[194] A. F. Pearce, "A structure, using resonant coupling elements, suitable for a high-power travelling-wave tube," *Proc. IEE*, vol. 105, pt. B, pp. 719–726; May, 1958.
[195] R. L. Pease, "On the propagation of surface waves over an infinite grounded ferrite slab," IRE TRANS. ON ANTENNAS AND PROPAGATION, vol. AP-6, pp. 13–20; January, 1958.
[196] R. W. Peter, J. A. Ruetz and A. B. Olson, "Attenuation of wire helices in dielectric supports," *RCA Rev.*, vol. 13, p. 558; 1952.
[197] R. S. Phillips, "The electromagnetic field produced by a helix," *Quart. Appl. Math.*, vol. 8, p. 229; 1950.
[198] G. Piefke, "On the theory of Harms-Goubau single-wire transmission lines for metre wavelengths," *Arch. elek. Übertragung*, vol. 9, p. 81; 1955.
[199] G. Piefke, "Wave propagation in a diaphragm-type and a corrugated waveguide," *Arch. elek. Übertragung*, vol. 12, p. 26; 1958.
[200] G. Piefke, "Reflection in helical lines at a change in the helix pitch," *Arch. elek. Übertragung*, vol. 9, pp. 269, 402; 1955.
[201] G. Piefke, "Wave propagation in a disk line," *Arch. elek. Übertragung*, vol. 11, p. 49; 1957.
[202] J. R. Pierce, "Circuits for travelling wave tubes," PROC. IRE, vol. 37, pp. 510–515; May, 1949.
[203] J. R. Pierce and P. K. Tien, "Coupling of modes in helices," PROC. IRE, vol. 42, pp. 1389–1396; September, 1954.
[204] J. R. Pierce, "Propagation in linear arrays of parallel wires," IRE TRANS. ON ELECTRON DEVICES, vol. ED-2, pp. 13–14; January, 1955.
[205] R. E. Plummer and R. C. Hansen, "Double-slab arbitrary-polarization surface-wave structures," *Proc. IEE*, vol. 104, pt. C, pp. 465–471; September, 1957.
[206] H. C. Pocklington, "Electrical oscillations in wires," *Proc. Cambridge Phil. Soc.*, vol. 9, p. 324; 1897.
[207] K. Pöschl, "Wave propagation along a helix with a cylindrical outer conductor," *Arch. elek. Übertragung*, vol. 7, p. 518; 1953.
[208] G. J. Rich, "The launching of a plane surface wave," *Proc. IEE*, pt. III, pp. 237–246; March, 1955.
[209] R. D. Richtmyer, "Dielectric resonators," *J. Appl. Phys.*, vol. 10, p. 391; 1939.
[210] T. E. Roberts, "Theory of the single-wire transmission line," *J. Appl. Phys.*, vol. 24, pp. 57–67; January, 1953.
[211] T. E. Roberts, "An experimental investigation of the single-wire transmission line," IRE TRANS. AND ANTENNAS AND PROPAGATION, vol. AP-2, pp. 46–56; April, 1954.
[212] P. N. Robson, "A note on the Fourier series representation of the dispersion curves for circular iris-loaded waveguides," *Proc. IEE*, vol. 105, pt. B, pp. 69–72; January, 1958.
[213] W. Rotman, "A study of single-surface corrugated guides," PROC. IRE, vol. 39, pp. 952–949; August, 1951.
[214] E. Roubine, "Investigation of electromagnetic waves guided by helical conductors," *Compt. Rend. Acad. Sci. (Paris)*, vol. 232, p. 1748; 1959; and, *Ann. Télécommun.*, vol. 7, pp. 206, 262, and 310; 1952.
[215] E. Roubine, "The helical circuit used in travelling wave tubes," *L'Onde Electrique*, vol. 27, p. 203; 1947.
[216] N. M. Rust, "Surface-wave transmission line," *Wireless Engr.*, vol. 27, p. 270; 1950.
[217] H. Ruter and O. Schriever, "Electromagnetic Waves in Dielectric Wires," Schriften Naturwissenschaften Verlag Schleswig-Holstein, Ger., vol. 16, p. 2; 1915.
[218] J. Saphores and L. Brillouin, "General properties of dielectric guides and cables," *Elec. Commun.*, vol. 16, p. 346; 1938.
[219] E. H. Scheibe, B. G. King, and D. L. Van Zeeland, "Loss measurements of surface-wave transmission lines," *J. Appl. Phys.*, vol. 25, pp. 790–797; June, 1954.
[220] S. A. Schelkunoff, "Electromagnetic Waves," D. Van Nostrand Co., Inc., New York, N. Y.; 1943.
[221] W. P. Schestopalow, "Theory of a waveguide containing a spiral, partly filled with a dielectric," *Nachr. Tech.*, vol. 4, p. 425, 1954; and *Zhur. Tekh. Fiz.*, vol. 22, p. 414, 1952.

[222] G. Schiefer, "The attenuation of the helical wire line," *Arch. elek. Übertragung*, vol. 11, p. 35; 1957.
[223] S. P. Schlesinger and D. D. King, "Dielectric image lines," IRE TRANS. ON MICROWAVE THEORY AND TECHNIQUES, vol. MTT-6, pp. 291–299; July, 1958.
[224] H. M. Schmidt, "Cylindrical surface-wave guides," *Z. Angew. Phys.*, vol. 3, p. 272; 1951.
[225] O. Schriever, "Electromagnetic waves in dielectric conductors," *Ann. Physik*, vol. 63, p. 645; 1920.
[226] G. Schulten, "Novel method for measuring impedance on surface-wave transmission lines," PROC. IRE, vol. 47, pp. 76–77; January, 1959.
[227] F. Sellberg, "Theoretical investigation of some closed delay structures for high-power travelling-wave tubes," *Proc. IEE*, vol. 105, pt. B, pp. 730–735; May, 1958.
[228] S. Sensiper, "Electromagnetic wave propagaiton on helical structures (a review and survey of recent progress)" PROC. IRE, vol. 43, pp. 149–161; February, 1955.
[229] R. Servant and P. Londette, "First results of a polarimetric study, with microwaves, of asymmetric metal resonators," *J. Phys. Radium*, vol. 14, p. 79S; 1953.
[230] K. P. Sharm, "An investigation of the excitation of radiation by surface waves," *Proc. IEE*, vol. 106, pt. B, pp. 116–122; March, 1959.
[231] C. E. Sharp and G. Goubau, "A UHF surface-wave transmission line," PROC. IRE, vol. 41, pp. 107–109; January, 1953.
[232] A. A. Sharshanov and K. N. Stepanov, "Electromagnetic wave propagation in an almost periodic waveguide," *Zhur. Tekh. Fiz.*, vol. 27, p. 1474; 1957.
[233] J. C. Slater, "Microwave Electronics," D. Van Nostrand Co. Inc., New York, N. Y.; 1950.
[234] K. E. Slevogt, "Propagation of decimetre waves along a dielectric line," *Hochfreq. und Elek.*, vol. 59, p. 1; 1942.
[235] W. Sichak, "Coaxial line with helical inner conductor," PROC. IRE, vol. 42, pp. 1315–1319; August, 1954.
[236] A. J. Simmons, "Phase shift by periodic loading of waveguide and its application to broad-band circular polarization," IRE TRANS. ON MICROWAVE THEORY AND TECHNIQUES, vol. MTT-3, pp. 18–21; December, 1955.
[237] N. N. Smirnov, "Propagation of waves along an infinitely long helix," *Compt. Rend. Acad. Sci. U.R.S.S.*, vol. 108, p. 243; 1956.
[238] N. N. Smirnov, "Dispersive properties of multifilar helices," *Compt. Rend. Acad. Sci. U.R.S.S.*, vol. 110, p. 212; 1956.
[239] V. Y. Smorgonskii, "Calculation of the phase and group velocity of surface waves," *Radiotekhnika*, vol. 10, p. 25; 1955.
[240] W. Sollfrey, "Wave propagation on helical wires," *J. Appl. Phys.*, vol. 22, pp. 905–910; July, 1951.
[241] E. G. Solov'ev, "Circular and rectangular waveguides with longitudinal diaphragms," *Zhur. Tech. Fiz.*, vol. 25, p. 707; 1955.
[242] E. G. Solov'ev, "Propagation of electromagnetic waves between two circular cylindrical surfaces in the presence of longitudinal periodically spaced diaphragms," *Radiotekhnika (Moscow)*, vol. 11, p. 57; 1956.
[243] E. G. Solov'ev and L. V. Belows, "Theory of helical line surrounded by a cylindrical semi-conducting envelope," *Radiotekhnika (Moscow)*, vol. 11, p. 31; 1956.
[244] A. Sommerfeld, "Propagation of electromagnetic waves along a cylindrical conductor," *Ann. Physik und Chemie*, vol. 67, p. 233; 1899.
[245] N. M. Sovetov, "Dispersion characteristic of a disk loaded waveguide," *Zhur. Tekh. Fiz.*, vol. 24, p. 1907; 1954.
[246] L. Stark, "Lower modes of a concentric line having a helical inner conductor," *J. Appl. Phys.*, vol. 25, pp. 1155–1162; September, 1954.
[247] H. Seyskal, "Experimental study of delay-lines," *L'Onde Electrique*, vol. 37, p. 86; 1957.
[248] J. A. Stratton, "Electromagnetic Theory," McGraw-Hill Book Co., Inc., New York, N. Y.; 1941.
[249] M. K. Subbarao and A. B. McLay, "Diffraction of 3.2 cm. electromagnetic waves by dielectric rods: part 1—lucite and tenite 1 in. diameter cylinders," *Can. J. Phys.*, vol. 34, p. 546; 1956.
[250] H. Suhl and L. R. Walker, "Topics in guided wave propagation through gyromagnetic media: part II—transverse magnetization and the nonreciprocal helix," *Bell Sys. Tech. J.*, vol. 33, pp. 939–986; July, 1954.
[251] D. T. Swift-Hook, "Dispersion curves for a helix in a glass tube," *Proc. IEE*, vol. 105, pt. B, pp. 747–755; May, 1958.
[252] P. K. Tien, "Traveling-wave-tube helix impedance," PROC. IRE, vol. 41, pp. 1617–1623; November, 1953.
[253] P. K. Tien, "Bifilar helix for backward wave oscillations," PROC. IRE, vol. 42, pp. 1137–1143; July, 1954.
[254] F. J. Tischer, "H-guide—a new microwave concept," *Electronic Ind. Tele-Tech.*, vol. 15, p. 50; 1956.
[225] F. J. Tischer, "H-guide, A waveguide for microwaves," 1956 IRE CONVENTION RECORD, pt. 5, pp. 44–47.
[256] S. E. Tsimring, "Variational calculation method for waveguides with periodic inhomogeneities: part 1," *Radiotekh. i Elektron.*, vol. 2, p. 3; 1957.
[257] H. Uchida and S. Nishida, "Surface and Space Waves on the Surface-Wave Transmission Line," Res. Insts., Tohuku University, Japan, Sci. Rept. 6B, p. 217; 1955.
[258] H. Uchida, S. Nishida, H. Uda, and H. Nagasawa, "The Shunt Reactive Element on the Surface-Wave Transmission line," Res. Insts., Tohuku University, Japan, Sci. Rept. 6B, p. 229; 1955.
[259] H. Uchida, S. Nishida, and H. Shioya, "Shielded Dielectric Waveguide," Res. Insts., Tohuku University, Japan, Sci. Rept. 8B, p. 7; 1956.
[260] K. Udagawa, "Propagation of electromagnetic waves in helical circuits coaxially surrounded by a dielectric tube," *J. Inst. Elec. Commun. Engrs. (Japan)*, vol. 35, p. 85; 1952.
[261] K. Udagawa, "On the attenuation characteristics of electromagnetic waves in helical circuits," *J. Inst. Elec. Commun. Engrs. (Japan)*, vol. 35, p. 342; 1952.
[262] T. Umehara, "Design charts for surface-wave transmission lines," *J. Inst. Elec. Commun. Engrs. (Japan)*, vol. 37, p. 425; 1954.
[263] H. G. Unger, "Transfer of energy by dielectric guides," *Fernmeldetech. Z.*, vol. 8, p. 438; 1955.
[264] H. G. Unger, "Dielectric tubes as waveguides," *Arch. elek. Übertragung*, vol. 8, p. 241; 1954.
[265] L. A. Vainshtein, "Surface electromagnetic waves on a comb structure," *Zhur. Tekh. Fiz.*, vol. 26, p. 385; 1956.
[266] S. A. Vakin, "Propagation of electromagnetic waves along an infinite helical slit," *Compt. Rend. Acad. Sci. U.R.S.S.*, vol. 84, p. 37; 1952.
[267] B. Valtersson, "Phase velocity in helical waveguides," *L'Onde Électrique*, vol. 37, p. 843; 1957.
[268] V. J. Vanhuyse, "On the (β_0, k) diagrams for circularly symmetric TM waves in infinite iris-loaded waveguides," *Nuovo Cim.*, vol. 1, p. 447; 1955.
[269] V. J. Vanhuyse, "On the proper frequencies of terminated waveguides," *Physica*, vol. 21, pp. 269, 603; 1955.
[270] V. J. Vanhuyse, "On the resonance frequencies and the field configurations in terminated corrugated waveguides," *Physica*, vol. 21, p. 829; 1955.
[271] R. E. Vowels, "Matrix methods in the solution of ladder networks," *J. IEE*, vol. 95, pp. 40–50; January, 1948.
[272] G. Wade and N. Rynn, "Coupled helices for use in travelling-wave tubes," IRE TRANS. ON ELECTRON DEVICES, vol. ED-2, pp. 15–24; July, 1955.
[273] J. R. Wait, "Excitation of surface waves on conducting stratified, dielectric-clad and corrugated surfaces," *J. Res. Natl. Bur. Standards*, vol. 59, p. 365; 1957.
[274] R. A. Waldron, "Theory of the helical waveguide of rectangular cross section," *J. Brit. IRE*, vol. 17, p. 577; 1957.
[275] R. A. Waldron, "A helical coordinate system and its applications in electromagnetic theory," *Quart. J. Mech. Appl. Math.*, vol. 11, pt. 4, pp. 438–461; November, 1958.
[276] J. C. Walling, "Interdigital and other slow wave structures," *J. Electronics*, vol. 3, p. 239; 1957.
[277] G. B. Walker and N. D. West, "Mode separation at the π-mode in a dielectric loaded waveguide," *Proc. IEE*, vol. 104, pt. C, pp. 381–387; September, 1957.
[278] G. B. Walker, "Dielectric loading for U.H.F. valves," *Proc. IEE*, vol. 105, pt. B, pp. 717–718; May, 1958.
[279] R. Warnecke, O. Doehler and P. Guenard, "On delay lines in the form of combs or interdigital structures and their equivalent circuits," *Compt. Rend. Acad. Sci. (Paris)*, vol. 231, p. 1220; 1950.
[280] D. A. Watkins and E. A. Ash, "The helix as a backward-wave circuit structure," *J. Appl. Phys.*, vol. 25, pp. 782–790; June, 1954.
[281] D. A. Watkins and A. E. Siegman, "Helix impedance measurements using an electron beam," *J. Appl. Phys.*, vol. 24, pp. 917–922, July, 1953; vol. 25, p. 133, January, 1954.
[282] W. H. Watson, "The experimental determination of equivalent networks for a coaxial line to helix junction," IRE TRANS. ON ELECTRON DEVICES, vol. ED-3, pp. 149–152; July, 1956.
[283] W. H. Watson and J. R. Whinnery, "Study of a plane short on a shielded helix," IRE TRANS. ON ELECTRON DEVICES, vol. ED-2, pp. 34–36; October, 1955.
[284] S. E. Webber, "Calculations of wave propagation of a helix in the attenuation region," IRE TRANS. ON ELECTRON DEVICES, vol. ED-1, pp. 35–39; August, 1954.

[285] H. Weber, "The dimensions of loaded waveguides for the H_{10} mode," *Telefunken Zeitung*, vol. 27, p. 44; 1954.
[286] M. T. Weiss and E. M. Gyorgy, "Low-loss dielectric waveguides," IRE TRANS. ON MICROWAVE THEORY AND TECHNIQUES, vol. MTT-2, pp. 38–44; September, 1954.
[287] R. E. White, "Coaxial-to-helix transducers for travelling-wavetubes," *Elec. Commun.*, December, 1953; also 1953 IRE CONVENTION RECORD, pt. 10, pp. 42–45.
[288] R. M. Whitmer, "Fields in nonmetallic waveguides," PROC. IRE, vol. 36, pp. 1105–1109; September, 1948.
[288a] E. Wild, "Electromagnetic waves in nearly periodic structures," *Quart. J. Mech. Appl. Math.*, vol. 10, p. 322; 1957.
[289] J. C. Wiltse, "Some characteristics of dielectric image lines at millimetre wavelengths," IRE TRANS. ON MICROWAVE THEORY AND TECHNIQUES, vol. MTT-7, pp. 65–69; January, 1959.
[290] H. Zahn, "Detection of electromagnetic waves in dielectric wires," *Ann. Physik*, vol. 49, p. 907; 1916.
[291] J. Zenneck, "On the propagation of plane electromagnetic waves along a flat conductor and its application to wireless telegraphy," *Ann. Physik*, vol. 23, p. 846; 1907.
[292] F. J. Zucker, "Theory and application of surface waves," *Nuovo Cim.*, vol. 9, (supplement), p. 450; 1952.
[293] F. J. Zucker, "The guiding and radiation of surface waves," *Proc. of the Symposium on Modern Advances in Microwave Techniques*, Polytechnic Inst. of Brooklyn, Brooklyn, N. Y.; 1954.

Design of Mode Transducers*

L. SOLYMAR† AND C. C. EAGLESFIELD†

Summary—**The propagation of the electromagnetic wave in a gradual transducer is discussed. It is shown that the incident mode and the geometry of the transducer determine the outgoing mode. Inverting this theorem, a method is suggested for the design of the transducer's surface for cases in which the desired modes in the uniform waveguides are given.**

The application of the method is illustrated in three examples.

I. INTRODUCTION

IN the design of a microwave transmission system it is often necessary to connect two uniform waveguides of different cross section by means of a nonuniform waveguide (subsequently referred to as a transducer). The transducer can be used for two different purposes: 1) to transform the same mode from one waveguide into another waveguide of different size; and 2) to transform a certain mode of one waveguide into a predetermined mode of the other waveguide.

The best example for the first type is a transducer between two rectangular waveguides of different size. The requirement is to transform efficiently the H_{01} mode in a specified bandwidth. All the solutions naturally employ a transducer whose cross section is everywhere rectangular. Similarly, the cross section of a transducer between two circular waveguides of different diameter is always circular. The problem in these cases is how to vary the size of the cross section. This field is well explored, and for certain cases optimum solutions have been obtained.

* Manuscript received by the PGMTT, July 6, 1959; revised manuscript received, August 17, 1959.
† Standard Telecommun. Labs. Ltd., Harlow, Essex, Eng.

The design of a transducer of the second type (generally called a mode transducer) is incomparably more complicated, since the shape of the cross section is varying. Although mode transducers have been used since the earliest days of microwave transmission, no systematic procedure seems to have been developed for the design of the required cross sections. The existing mode transducers were designed by physical intuition.

The aim of the present paper is to suggest a systematic design method. For the better understanding of the basic phenomena, the properties of a given transducer are first analyzed. It is shown that the incident mode and the surface of a sufficiently gradual transducer determine the outgoing mode. In the third section the inverse problem is dealt with, *i.e.*, choosing the surface of the transducer when the desired modes in the uniform waveguides are given.

II. THE PROPAGATION OF THE ELECTROMAGNETIC WAVE IN A SUFFICIENTLY GRADUAL TRANSDUCER

Let us consider the following arrangement of waveguides (see Fig. 1). The uniform waveguide A extends from $z = -\infty$ to $z = 0$, the transducer from $z = 0$ to $z = L$ and the uniform waveguide B from $z = L$ to $z = \infty$.

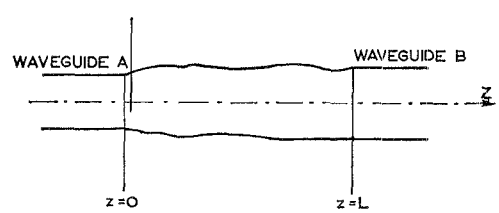

Fig. 1.